

AD-A047 257

VARIAN ASSOCIATES PALO ALTO CALIF
LONG PULSE HIGH EFFICIENCY SWITCH TUBE DEVELOPMENT.(U)
SEP 77 D BOILARD

F/G 9/1

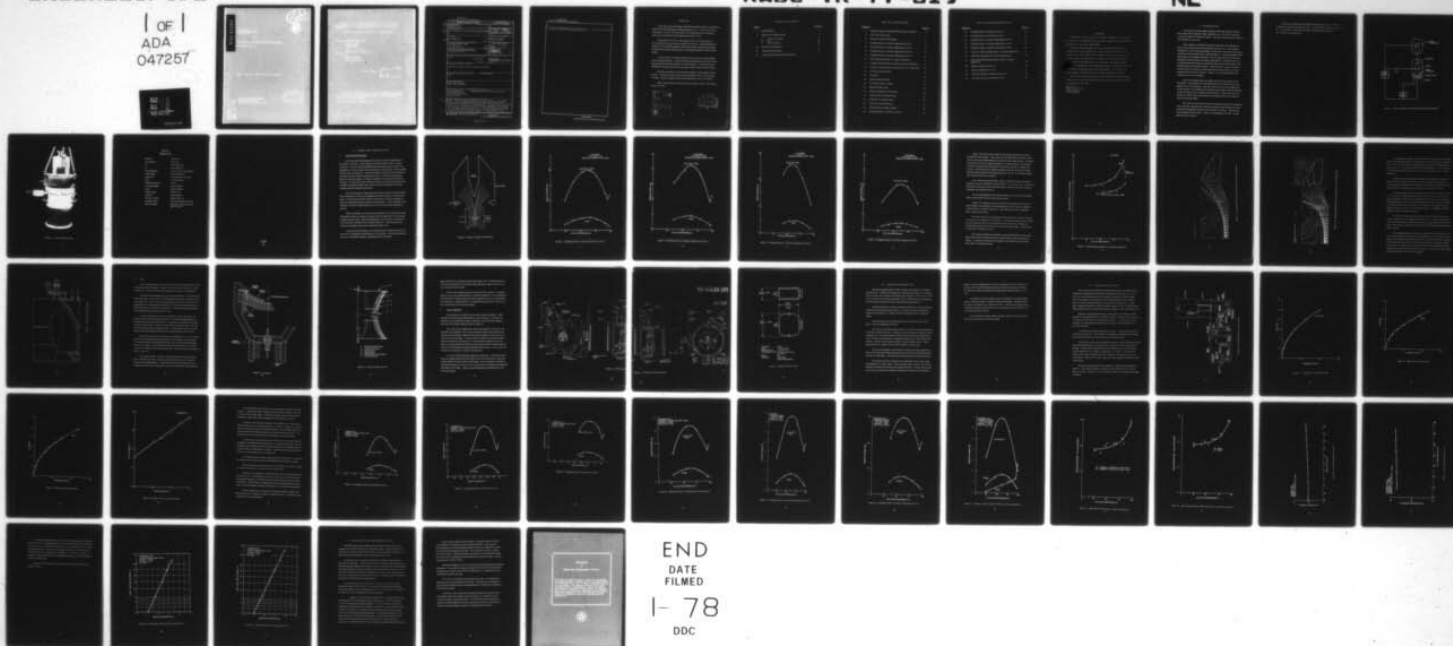
UNCLASSIFIED

RADC-TR-77-319

F30602-76-C-0259

NL

1 OF 1
ADA
047257



END
DATE
FILMED
1-78
DOC

END
DATE
FILMED
1-78
DOC

END
DATE
FILMED
1-78
DOC

END
DATE
FILMED
1-78
DOC

END
DATE
FILMED
1-78
DOC

AD A0 47257

UNCLASSIFIED

SECURITY CLASSIFICATION OF THIS PAGE (When Data Entered)

19 REPORT DOCUMENTATION PAGE		READ INSTRUCTIONS BEFORE COMPLETING FORM	
18 1. REPORT NUMBER RADC-TR-77-319 ✓	2 GOVT ACCESSION NO.	3 RECIPIENT'S CATALOG NUMBER 7	
6 4. TITLE (and Subtitle) LONG PULSE HIGH EFFICIENCY SWITCH TUBE DEVELOPMENT	5. TYPE OF REPORT & PERIOD COVERED Final Technical Report. 13 May 1976 - 30 June 1977		
	6. PERFORMING ORG. REPORT NUMBER N/A		
10 7. AUTHOR(s) Dennis/Boilard	15 8. CONTRACT OR GRANT NUMBER(s) F30602-76-C-0259 new		
9. PERFORMING ORGANIZATION NAME AND ADDRESS Varian Associates, Inc. ✓ 611 Hansen Way Palo Alto CA 94303	16 10. PROGRAM ELEMENT, PROJECT, TASK AREA & WORK UNIT NUMBERS 62702F 45060361 17 43		
11 11. CONTROLLING OFFICE NAME AND ADDRESS Rome Air Development Center (OCTP) Griffiss AFB NY 13441	12 REPORT DATE September 1977		
	13. NUMBER OF PAGES 53		
14. MONITORING AGENCY NAME & ADDRESS (if different from Controlling Office) Same	15. SECURITY CLASS. (of this report) UNCLASSIFIED		
	15a. DECLASSIFICATION/DOWNGRADING SCHEDULE N/A		
16. DISTRIBUTION STATEMENT (of this Report) Approved for public release; distribution unlimited.			
17. DISTRIBUTION STATEMENT (of the abstract enter) Same 20. If different from Report)			
18. SUPPLEMENTARY NOTES RADC Project Engineer: Albert Morreall (OCTP)			
19. KEY WORDS (Continue on reverse side if necessary and identify by block number) Linear-beam tetrode Voltage-depressible collector-probe system Nonintercepting grid Convergent electron beam High efficiency			
20. ABSTRACT (Continue on reverse side if necessary and identify by block number) This Report covers the design, fabrication and initial testing of a linear beam tetrode switch tube developed by Varian for RADC. Earlier models were developed by Varian under Air Force sponsorship. Design goals were 140 kV video output at 100 A load current and 0.08 (0.03 min) duty cycle at pulse lengths up to 300 μsec. Important features are the nonintercepting grid, convergent electron beam passing through the anode (screen grid), high efficiency, and voltage-depressible collector-probe system. Cooling capability of the collector and probe was improved through a new, computer-aided thermal design			

DD FORM 1 JAN 73 1473

EDITION OF 1 NOV 65 IS OBSOLETE

UNCLASSIFIED

SECURITY CLASSIFICATION OF THIS PAGE (When Data Entered)

MICROSEC

364 100

not

UNCLASSIFIED

SECURITY CLASSIFICATION OF THIS PAGE(When Data Entered)

which retained approximately the same geometry. The collector-probe system was evaluated up to 100 kV video output at 0.03 duty.

UNCLASSIFIED

SECURITY CLASSIFICATION OF THIS PAGE(When Data Entered)

SUMMARY

This report covers the design, fabrication and initial testing of a linear beam tetrode switch tube developed by Varian Associates, Inc., for Rome Air Development Center, New York. Earlier models of the switch tube were developed by Varian on work sponsored by the Department of the Air Force.

Design goals were 140 kV video output at 100 A load current and 0.08 (0.03 minimum) duty cycle at pulse lengths up to 300 μ sec. Important features of the tube are the nonintercepting grid, convergent electron beam passing through the anode (screen grid), high efficiency, and voltage-depressible collector-probe system.

A primary task of the present program was to improve cooling capability of the collector and probe. An improved thermal design was devised while retaining approximately the same geometry as used previously. Calorimetric experiments with an earlier tube as well as computer analysis aided in the new design.

The tube was tested up to the maximum capability of the available Varian test set. The collector-probe system was evaluated up to 100 kV video output at 0.03 duty. Dynamic impedance and grid characteristics were also measured.

Future testing of the tube will be under the direction of Mr. Al Morreall at RADC, New York.

ASSIGNMENT FOR	
NTIS	White Section <input checked="" type="checkbox"/>
DDC	Buff Section <input type="checkbox"/>
UNANNOUNCED	<input type="checkbox"/>
JUSTIFICATION	
BY	
DISTRIBUTION/AVAILABILITY CODES	
Dist.	AVAIL. and/or SPECIAL
A	

DDC
RECEIVED
DEC 5 1977
D

TABLE OF CONTENTS

<u>Section</u>	<u>Page No.</u>
I. INTRODUCTION.	1
II. DESIGN AND CONSTRUCTION	7
A. Collector and Probe	7
B. Gun	19
C. Final Assembly.	22
III. EXHAUST AND HIGH POT.	25
IV. PRELIMINARY TESTING	27
V. CONCLUSIONS AND RECOMMENDATIONS.	49

LIST OF ILLUSTRATIONS

<u>Figure No.</u>		<u>Page No.</u>
1.	Schematic Diagram Tetrode Switch Tube Series Modulator. .	3
2.	VKW-8253C Switch Tube	4
3.	Sketch of Collector-Probe Region	8
4.	Dissipated Power vs Collector Depression at 88 kV. . . .	9
5.	Dissipated Power vs Collector Depression at 108 kV . . .	10
6.	Dissipated Power vs Collector Depression at 108 kV . . .	11
7.	Dissipated Power vs Collector Depression at 90 kV. . . .	12
8.	VKW-8253B Probe Power vs Collector Depression	14
9.	Computer Printout Electron Trajectories at 90% Depression .	15
10.	Computer Printout Electron Trajectories at 95.2% Depression	16
11.	Collector-Probe Assembly	18
12.	Gun Sketch	20
13.	Heater Package Assembly	21
14.	VKW-8253C Outline Drawing	23
15.	Shielded VacIon® Pump	24
16.	Simplified Modulator Layout Sketch	28
17.	Collector Flow vs Pressure Drop	29
18.	Probe Flow vs Pressure Drop	30
19.	Body Flow vs Pressure Drop	31
20.	Heater Current vs Heater Voltage	32
21.	Dissipated Power vs Grid Drive at 69 kV	34

LIST OF ILLUSTRATIONS (Cont.)

<u>Figure No.</u>		<u>Page No.</u>
22.	Dissipated Power vs Grid Drive at 87 kV	35
23.	Dissipated Power vs Grid Drive at 99 kV	36
24.	Dissipated Power vs Collector Depression at 69 kV	37
25.	Dissipated Power vs Collector Depression at 88 kV	38
26.	Dissipated Power vs Collector Depression at 99 kV	39
27.	Collector, Probe, and Body Power vs Collector Depression	40
28.	VKW-8253C Probe Power vs Collector Depression	41
29.	VKW-8253B and VKW-8253C Probe Power vs Collector Depression	42
30.	Dynamic Impedance at 63.5 kV	43
31.	Dynamic Impedance at 72.3 kV	44
32.	Load Tube Current vs Grid Drive at 69.3 kV	46
33.	Load Tube Current vs Grid Drive at 87 kV	47

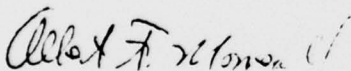
EVALUATION

The purpose of this effort was the design, development, fabrication and testing of a linear beam hard tube switch destined for series modulator application in high power radar systems.

Among the many advantages this type of modulation provides over conventional switching methods are: higher power and efficiency, protection of the final amplifier in the event of arcing in either the load or switch tubes, and the ability to control the pulse width and shape.

The unique characteristics will be of utmost importance to ECCM and MTI work proposed for future high power tactical systems which will be subjected to increasingly hostile ECM environments. This work is in direct support of RADC Technology Plan TPO-1B (Surveillance ECCM).

The success of this program and recent developments in high voltage technology have indicated that further work in this area would be fruitful at comparatively low risk.



ALBERT MORREALL
Project Engineer

I. INTRODUCTION

This report covers the design, fabrication and initial testing of a linear-beam switch tube developed by Varian Associates, Inc., Palo Alto, California, on contract F30602-76-C-0259, for RADC. The program was initiated in May 1976 and completed in June, 1977.

Early models of the linear-beam tetrode switch tube were developed by Varian on work sponsored by the Department of the Air Force. The design is specifically for series cathode modulation of linear-beam microwave tubes having an electron beam micropervance of approximately 2.0. Important features of the switch tube are the nonintercepting grid, the convergent electron beam passing through the grounded anode (screen grid), high efficiency resulting from the controlled spreading of the beam as it enters the region of the collector (plate), and the depressible collector-probe system. When the beam traverses the anode to collector space, the collector is depressed toward cathode potential causing an equivalent current to flow in the load. Figure 1 is a schematic diagram of the switch tube as a series modulator.

Prior to the present effort, the latest model of the switch tube was the VKW-8253B. The ratings of the VKW-8253B are 135 kV dc holdoff with a video output of 120 kV at 83 amperes. Duty cycle rating is 0.02 at pulse lengths up to 55 microseconds. The switch tube is operated near the highest possible efficiency in order to minimize power dissipation in the collector. When operating as described, the VKW-8253B is performing near its designed limits with respect to duty cycle and pulse length.

The objective of the present work was to design and fabricate a breadboard model long pulse, high efficiency switch tube generally patterned after the tetrode switch tube developed by Varian under earlier Air Force efforts. The tube has been designated the VKW-8253C. Figure 2 is a photograph of the tube. Design goals are given in Table 1.

Preliminary testing was performed at Varian Associates, Inc., Palo Alto California, in late May and early June 1977. It was delivered to RADC, Griffiss AFB N.Y., in June 1977. Future use of the tube will be under the direction of Mr. Al Morreall of that facility.

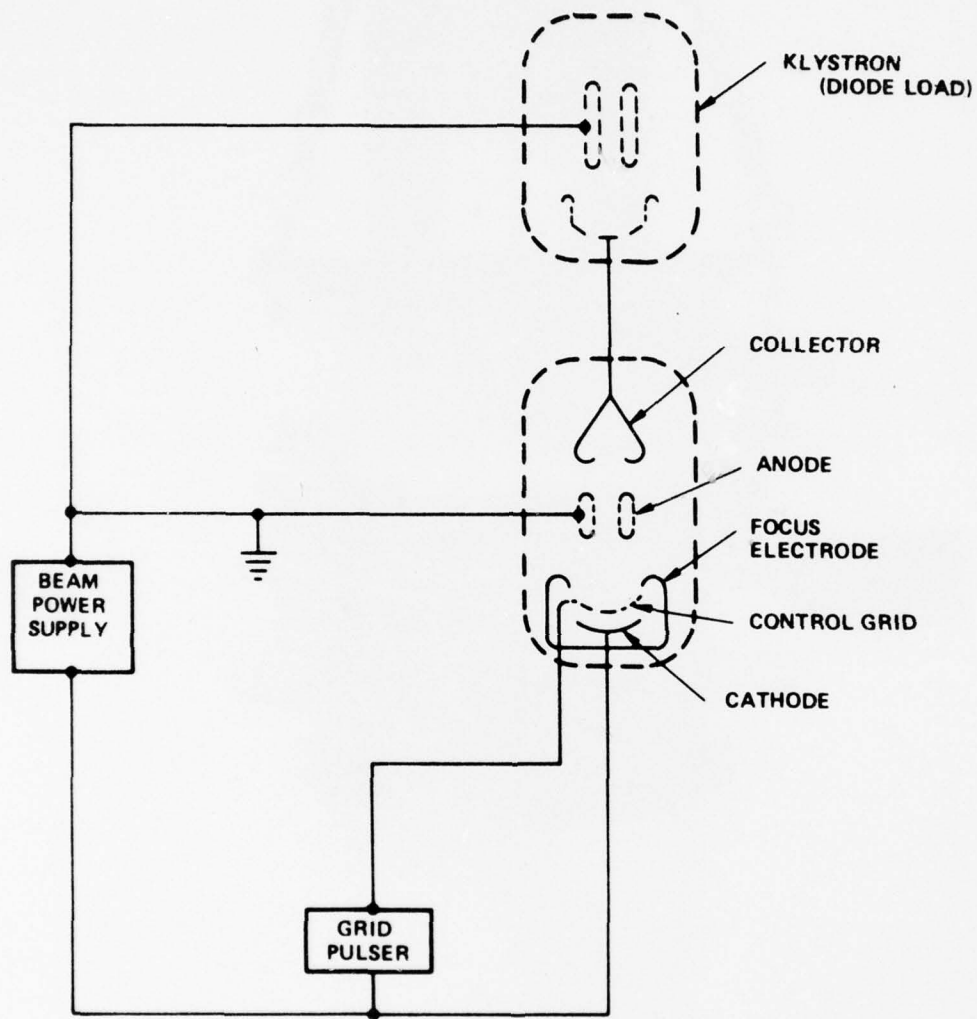


Figure 1. Schematic Diagram Tetrode Switch Tube Series Modulator

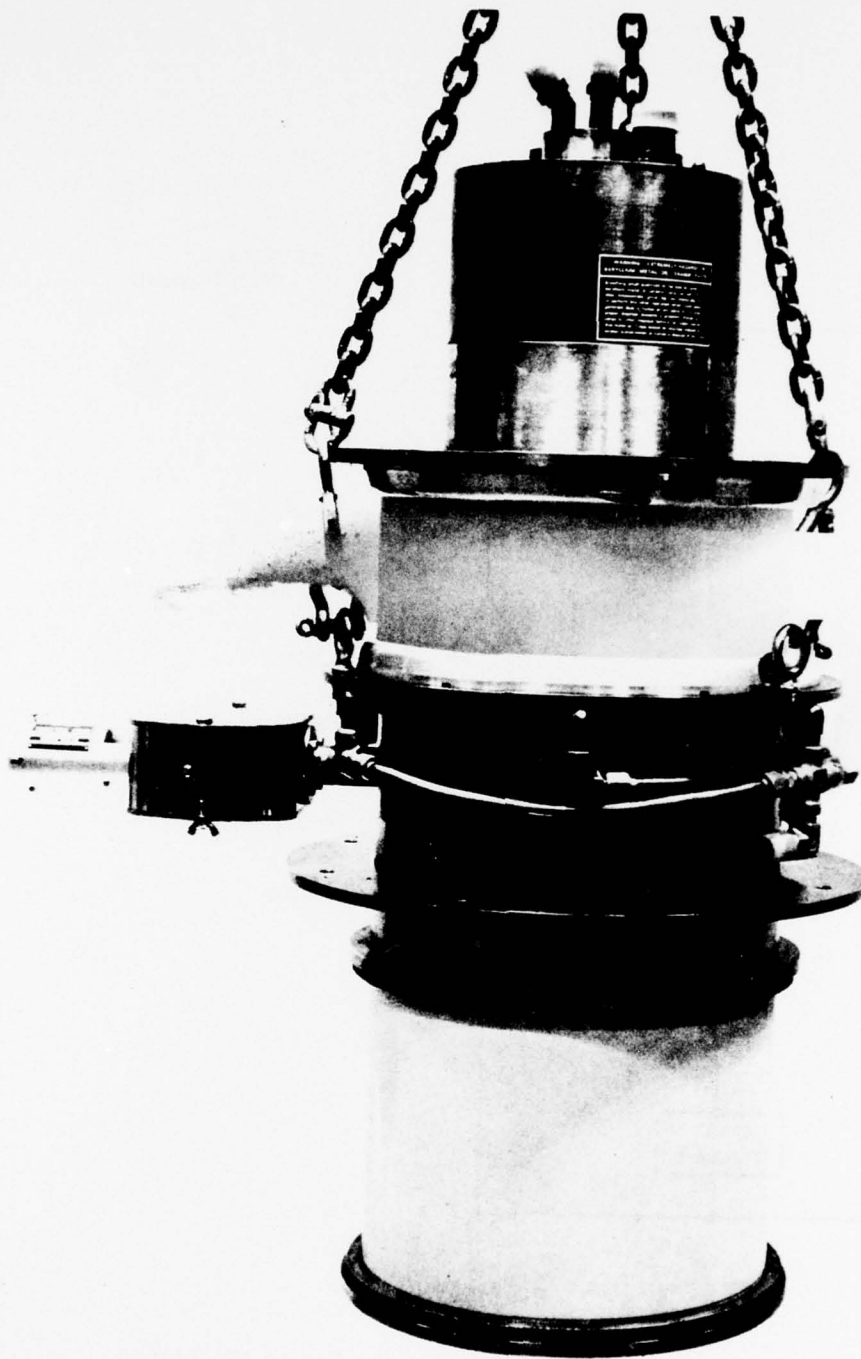


Figure 2. VKW-8253C Switch Tube

TABLE 1
DESIGN GOALS

Hold off	165 kV dc
DC operation	155 kV dc
E_c	140 kV video out
I_c	100 A video out
Load impedance	1.6 to 2.0 μ perv (perveance)
Pulse length	300 microseconds
Duty cycle	0.03 minimum, 0.08 goal
Bias	1.5 kV minimum
Positive grid drive	3.5 kV
Grid interception	5% I_b maximum
Anode	Ground potential
Anode cooling	Water or oil
Collector	Video potential
Collector cooling	Water and/or oil
Appendage pump	Ion pump attached to the tube
Size and weight	Minimum consistent with the state of the art

blank
6

II. DESIGN AND CONSTRUCTION

A. COLLECTOR AND PROBE

A primary task of this program was to improve the cooling capability of the collector and probe. A line drawing of the probe-collector region is shown in Figure 3. Earlier work had established that the optimum anode-collector configuration was a mirror image of the electron gun-to-anode region, with the cathode replaced with a central probe. The flytrap captures a portion of the returned electrons that otherwise would be returned to the anode. Particular emphasis was placed on the probe design as it contains considerably less surface area than the collector. Our plan was to retain the basic collector and center probe system used on earlier switch tube models, since it offers the best combination of minimum voltage gradient and space-charge control.

Early in the program, experiments were performed with the existing switch tube to determine the division of dissipated beam power between the collector and probe. Coolant to the probe and collector circuits was controlled separately so that power dissipated could be measured calorimetrically. Power measured in the collector circuit also included body power as its cooling circuit was plumbed in parallel.

Figures 4 through 7 are plots of power dissipated in the collector and probe sections of the tube as a function of percent collector depression for several beam voltages and duty cycles. Beyond 95% depression, the body power increases rapidly with further depression due to reflected electrons. This accounts for the increase of dissipated power on the collector plus body curve.

Maximum power dissipation in the collector probe combination occurs at a grid drive corresponding to approximately 60% depression. This result was expected from a mathematical analysis, ignoring second order effects.

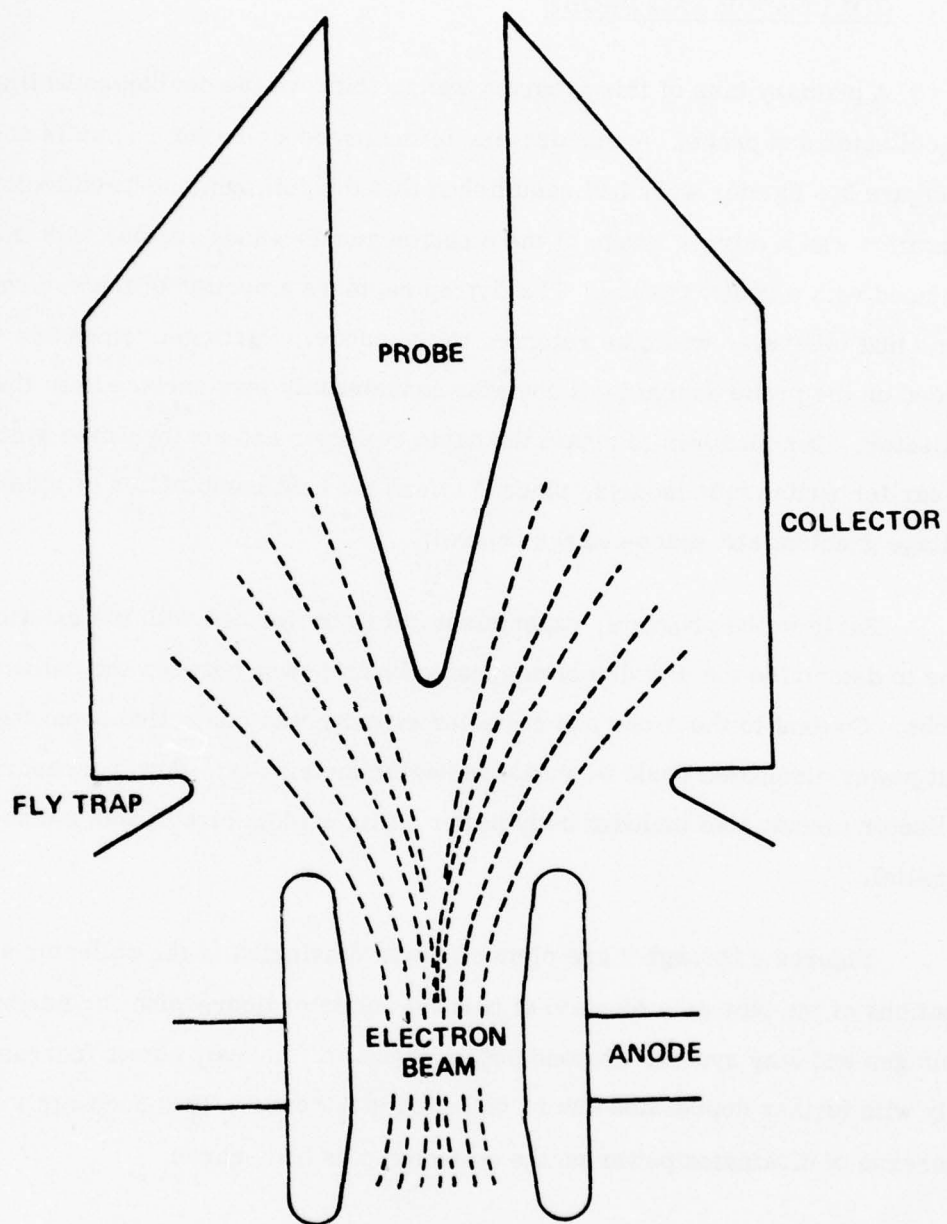


Figure 3. Sketch of Collector-Probe Region

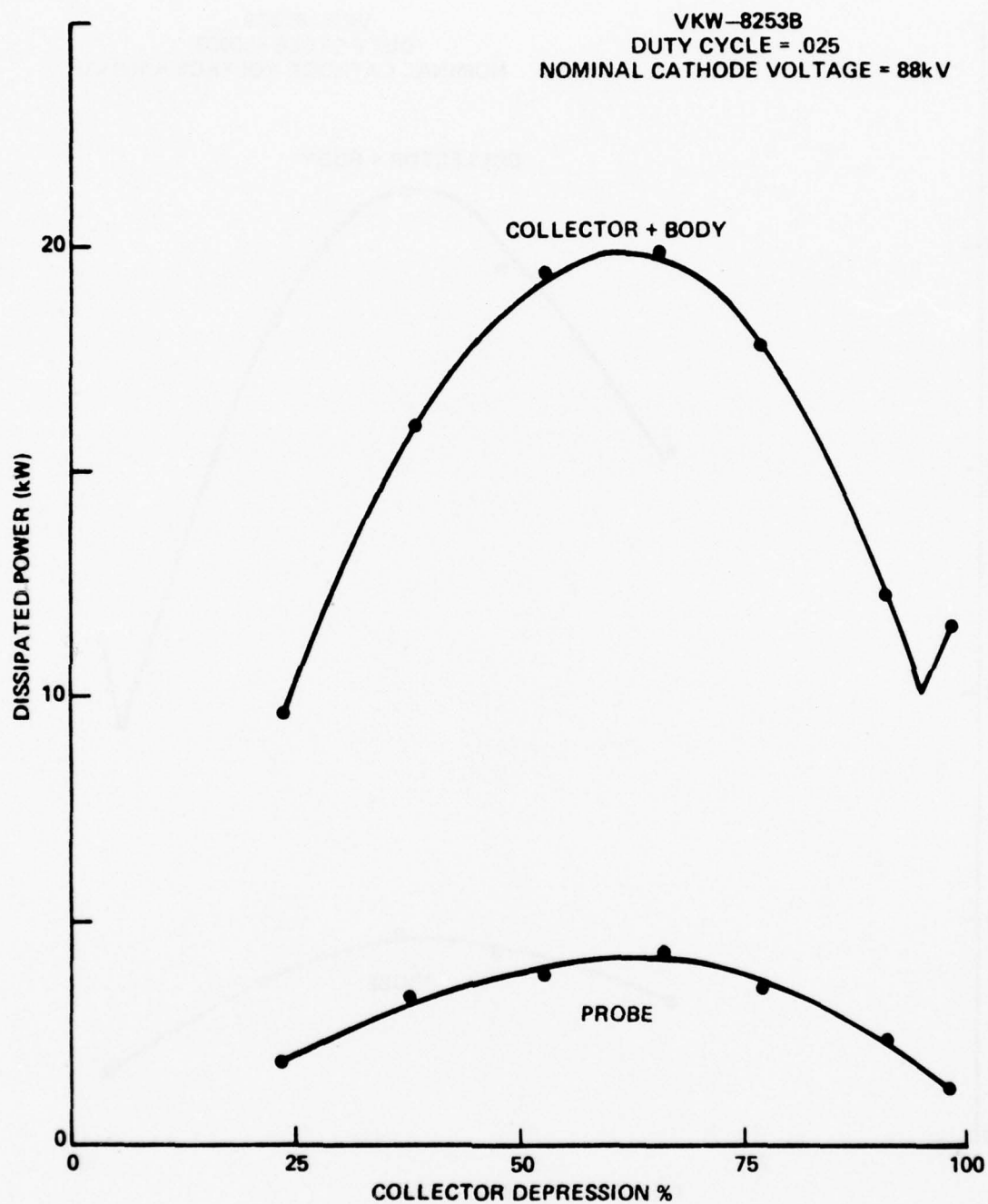


Figure 4. Dissipated Power vs Collector Depression at 88 kV

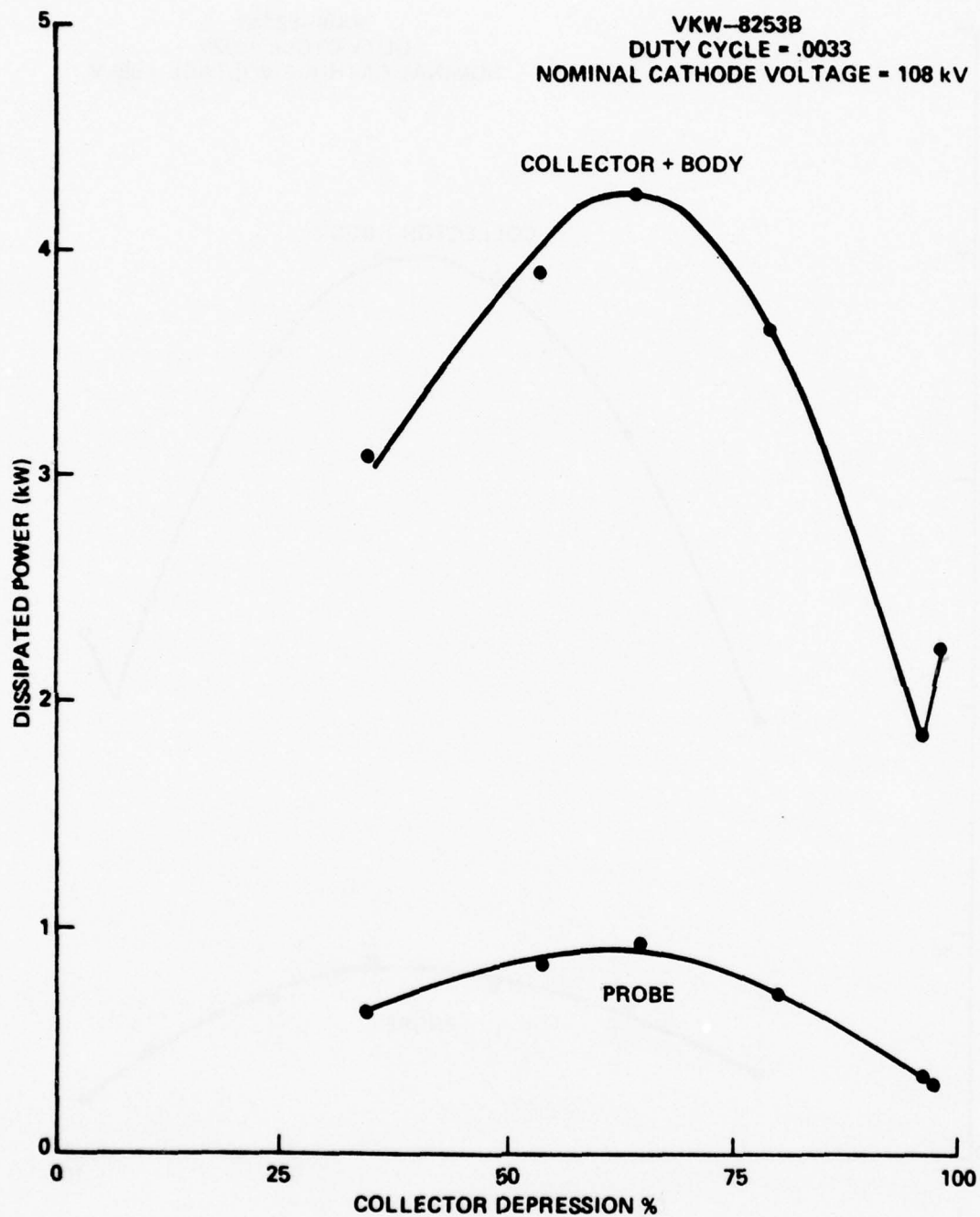


Figure 5. Dissipated Power vs Collector Depression at 108 kV

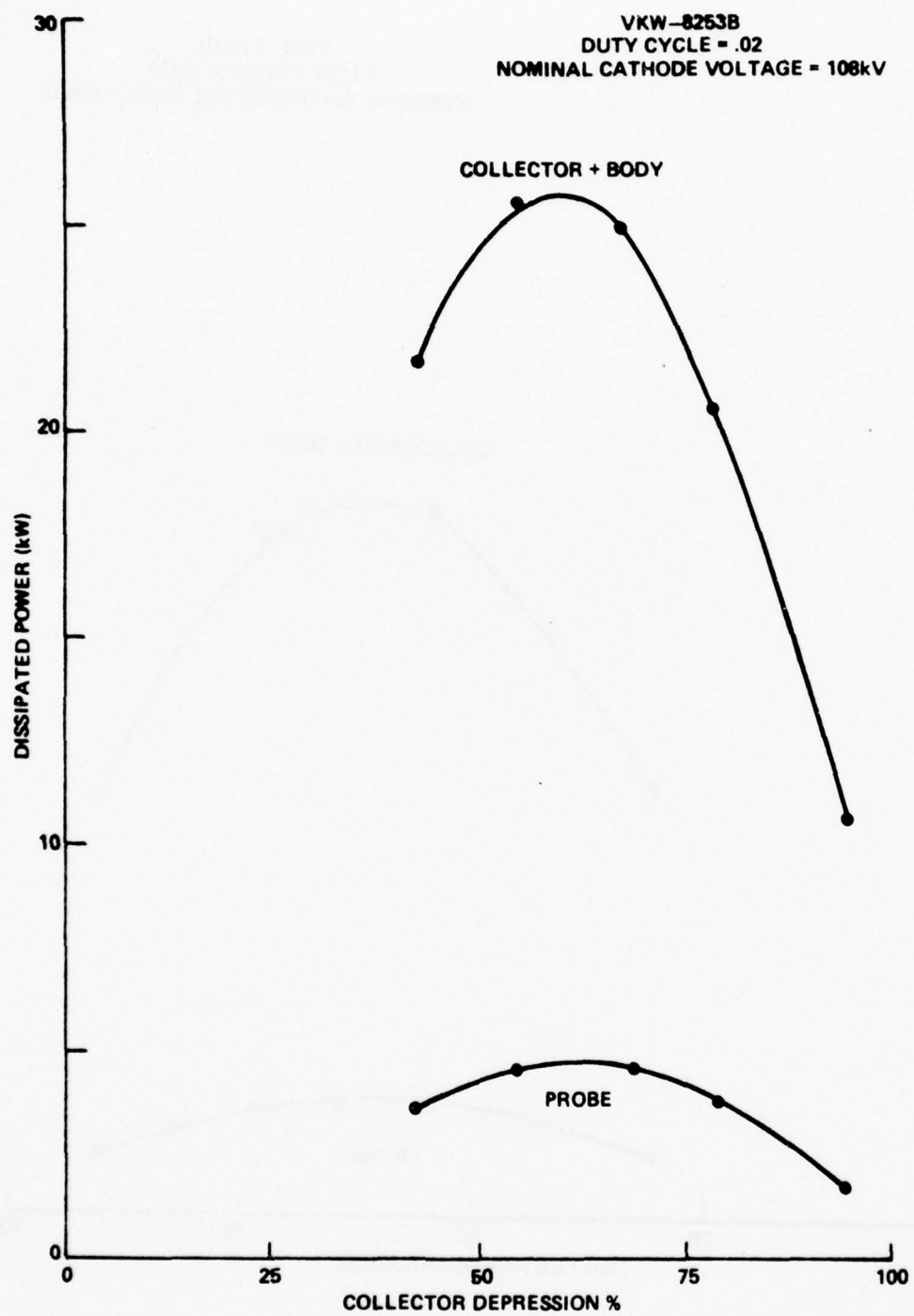


Figure 6. Dissipated Power vs Collector Depression at 108 kV

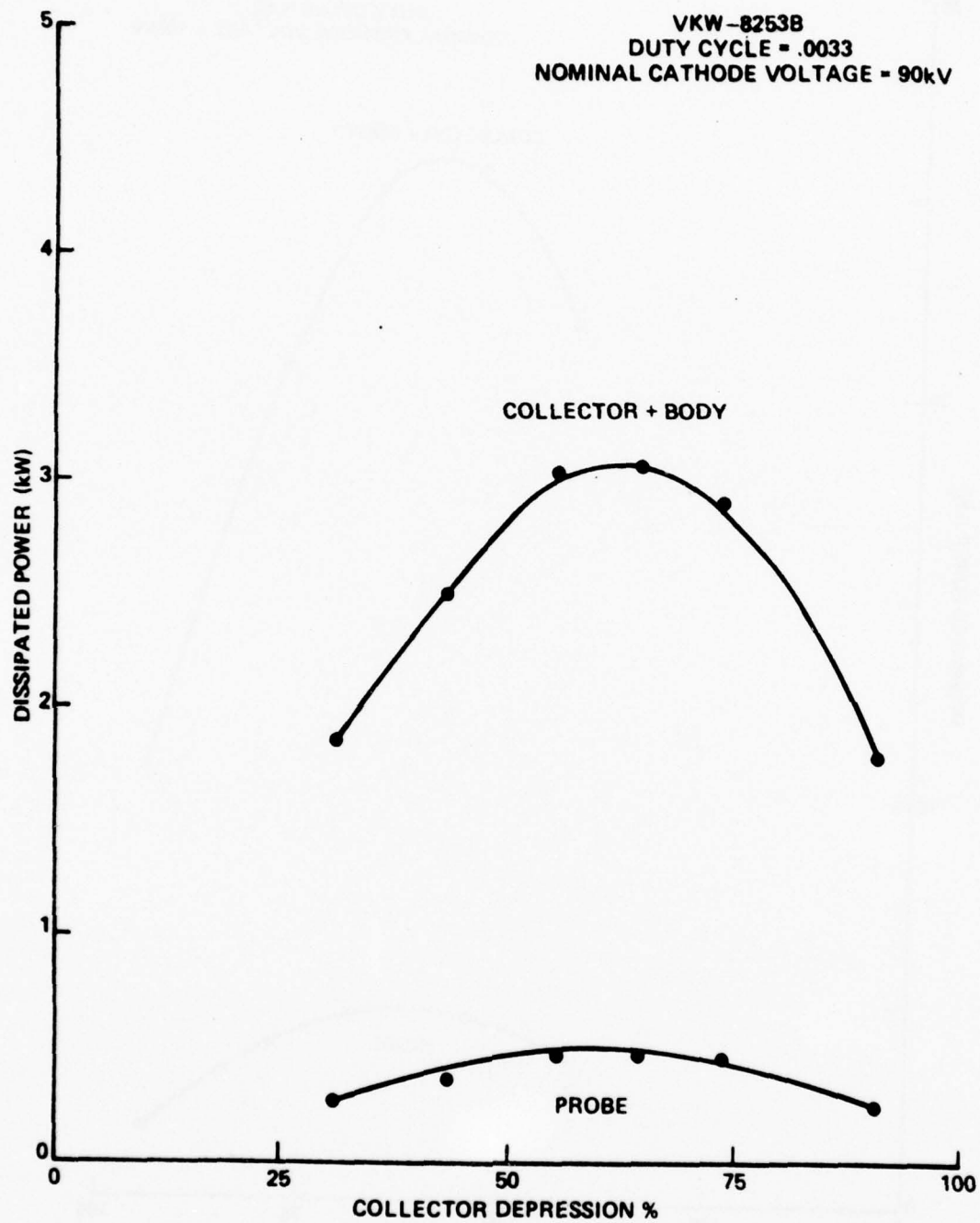


Figure 7. Dissipated Power vs Collector Depression at 90 kV

Figure 8 shows the ratio of probe to total (probe plus collector) power at two different beam voltages. Total power was calculated from the product of load current, duty cycle and the difference of beam and video output voltage. Also shown is the ratio predicted by computer analysis on an earlier program. At the point of preferred operation (approximately 90% depression) the ratio is between 0.20 and 0.28. Experiments under different operating conditions had similar results with data points generally falling between these two curves. The computer predicted a ratio between the two extremes.

Above 95% depression, the ratio of probe to total power increased rapidly, although the absolute magnitude of probe power was still decreasing. Operation at such extreme depression levels should be avoided, however, because of problems associated with reflected electrons.

The information gained in the course of these experiments formed the foundation for proceeding with the collector-probe design.

Initially, the computer was used to study electron trajectories in the collector region for two different probe configurations at 155 kV cathode voltage and various degrees of collector depression. Later studies were done at different beam voltages and currents.

The electron beam profile predicted by the Electron Gun Computer Program was used as the starting point in our analysis. The spreading electron beam caused by the decelerating effect of the depressed collector potential was obtained by launching the predicted initial beam into the collector-probe region. Typical printouts are shown in Figures 9 and 10.

The computer analysis provided data to make approximations of power density profiles along the probe and collector surfaces under various operating conditions. As expected, predicted power densities are greatest near the tip of the probe under all conditions studied.

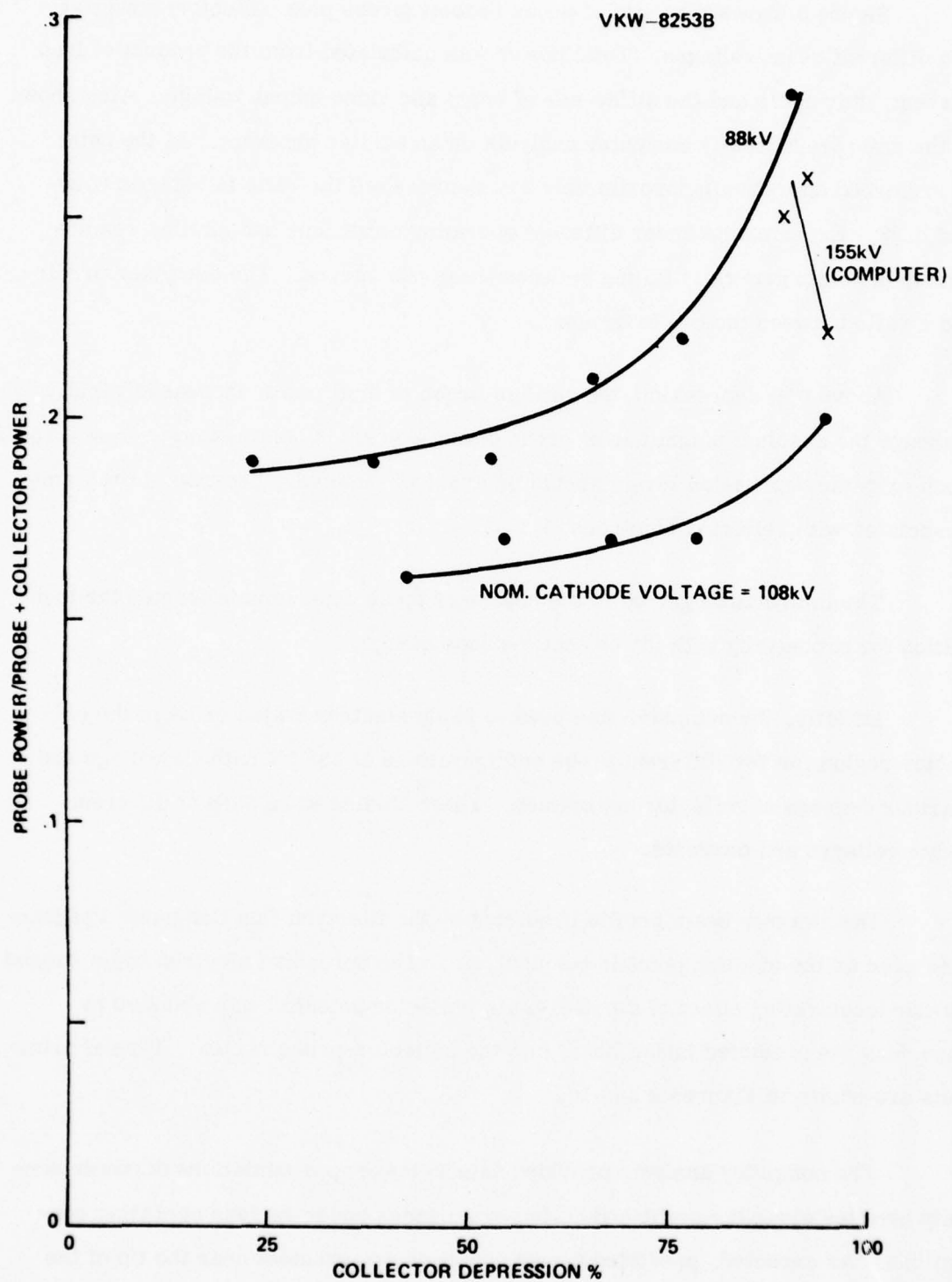


Figure 8. VKW-8253B Probe Power vs Collector Depression

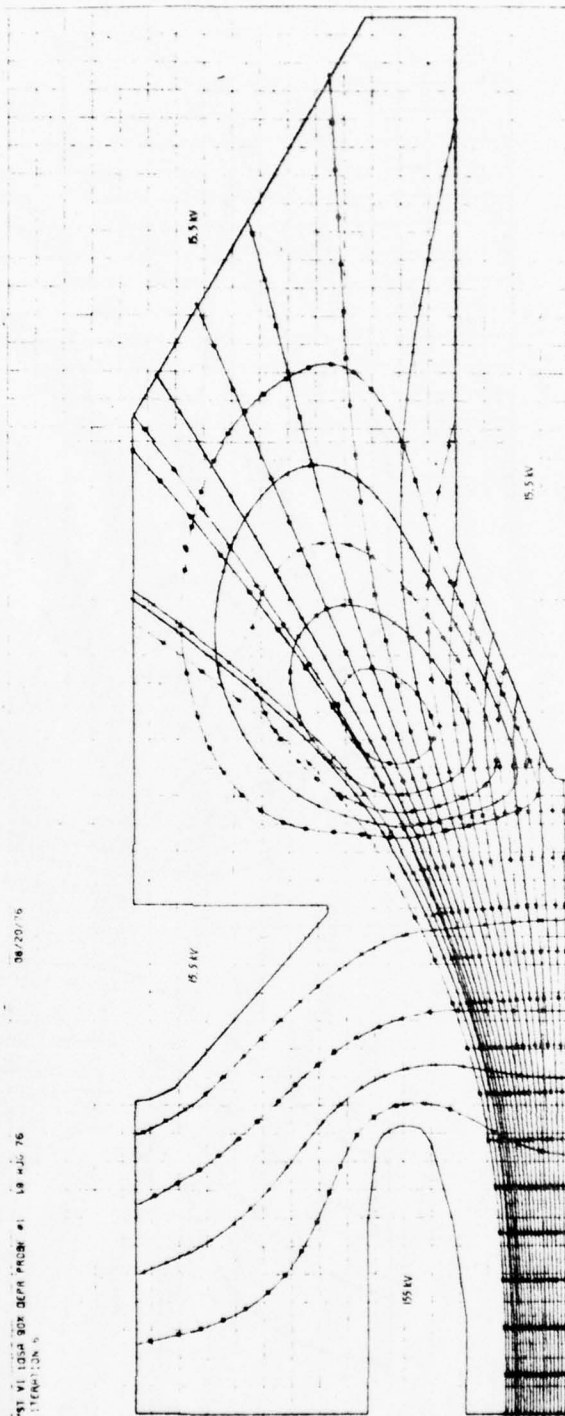


Figure 9. Computer Printout Electron Trajectories at 90% Depression

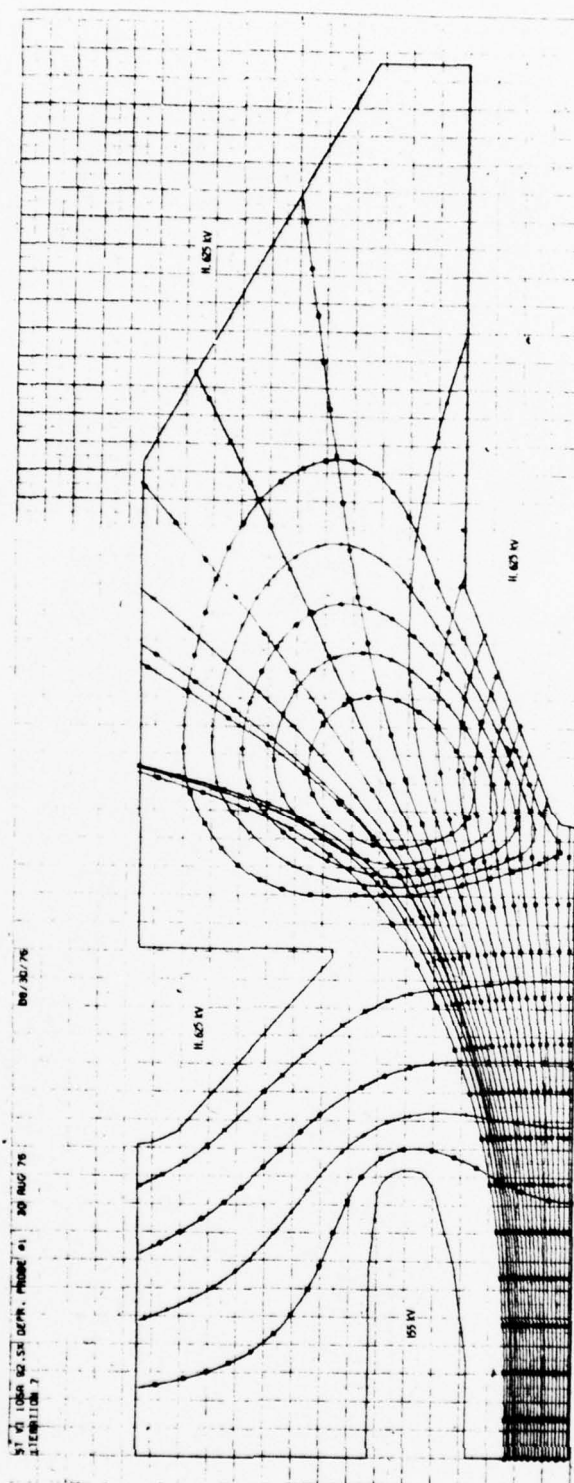


Figure 10. Computer Printout Electron Trajectories at 92.5% Depression

At constant beam voltage, the predicted percent of total collector and probe surface area experiencing direct beam interception varied with current and depression. At 155 kV, 105 A and 92 1/2% depression, the ratio of intercepted area to total area is 0.83. The ratio drops to 0.73 at 90% depression. At 155 kV and 120 A corresponding interception ratios are 0.9 at 92 1/2% depression and 0.77 at 90% depression.

These data, along with solutions at different combinations of beam parameters, aided in evaluation of the several tentative collector-probe designs. It was recognized that exact beam trajectories will be further influenced by such factors as initial beam diameter, gas ion focusing, and secondary electrons.

A drawing of the collector-probe assembly decided upon is shown in Figure 11. The probe is cylindrical except for a two-inch taper in the region of initial beam interception. High-velocity coolant enters the probe tip from a sump located along the probe center line. The coolant spirals along the length of the probe in a channel within the wall of the probe. All elements of the probe and cooling baffle are made of copper for maximum heat transfer. Five-eighths inch flare fittings are used on the probe manifolds.

The collector configuration decided upon consists of three principal elements: beam entrance lip, cylindrical section, and cone. The lip captures secondary and reflected electrons that otherwise would be accelerated toward the tube body. It also forms a useful cross-over channel for returning coolant water to the outlet manifold.

The straight portion of the collector is a thick-wall copper cylinder. Parallel coolant channels are formed by drilling longitudinal 0.187" diameter holes in the wall. The end cone is finned so that a groove aligns with each hold. Entering coolant floods one-half of the cone, flows along the grooves and into the drilled holes in that 180° sector, turns around in the lip at the beam entrance and flows through the parallel holes in the water return sector. The collector coolant manifolds are fitted with one-inch male pipe nipples.

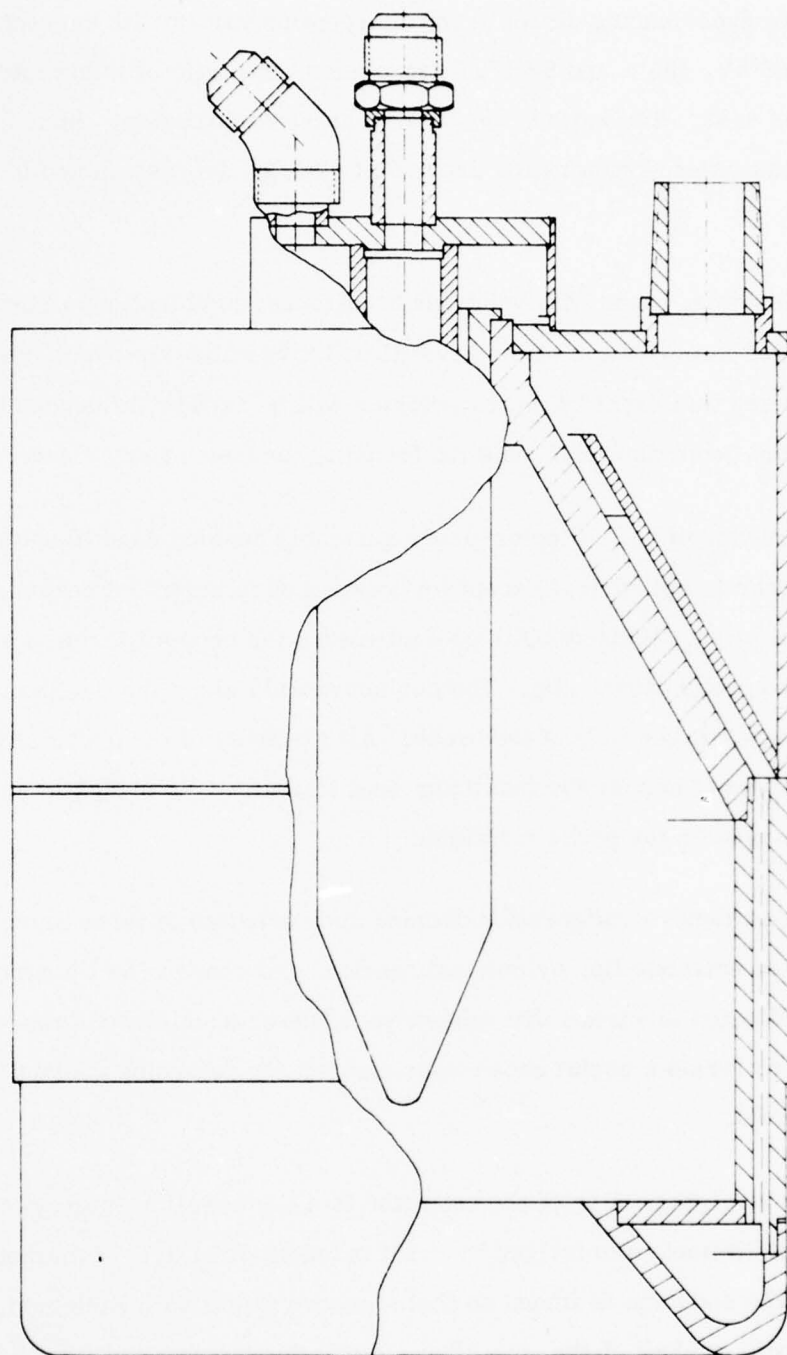


Figure 11. Collector-Probe Assembly

B. GUN

Major elements of the gun are the control grid, cathode-shadow grid, heater package and support structure. A sketch of the gun is shown in Figure 12. Internal gun parts were vacuum fired at high temperature just prior to assembling.

The control grid is supported by 32 beryllium-oxide rods. Each of the insulators was brazed on one end to the molybdenum grid blank and on the other end to a mounting plate. After brazing, the grid pattern was formed in the blank by electrical-discharge machining (EDM) techniques. The grid was electropolished as a final step to attain an extremely smooth finish. One assembly developed cracks in the molybdenum during EDM and was not usable.

A nickel-cathode button was formed, blanked and finish machined. 125 dimples were machined on the button surface to provide the emitting surface for the beamlets that form the electron beam. Nickelating was applied to each dimple and sinter fired in place. Just prior to sealing into the final assembly, each dimple was coated with barium triple carbonate. A nickel shadow grid was carefully aligned with the dimples and attached to the cathode button as a final process.

The heater was wound of 0.060 diameter molybdenum wire. After winding, the heater was sandblasted to insure adhesion of the "Rockide" ceramic coating. The completed heater was nested between two concave heat shields and hydrogen fired to set its shape. When assembled into the heat-shield package, the heater conforms to the dished back of the cathode button. The heater package assembly is shown in Figure 13.

The support structure consists of a truncated copper cone brazed at one end to a stainless steel tube. Copper cooling fins are located in the vicinity of the grid feed-through insulator. A baffle was added after tube exhaust to form a cooling circuit such that oil can be pump-forced over the fins and return down the

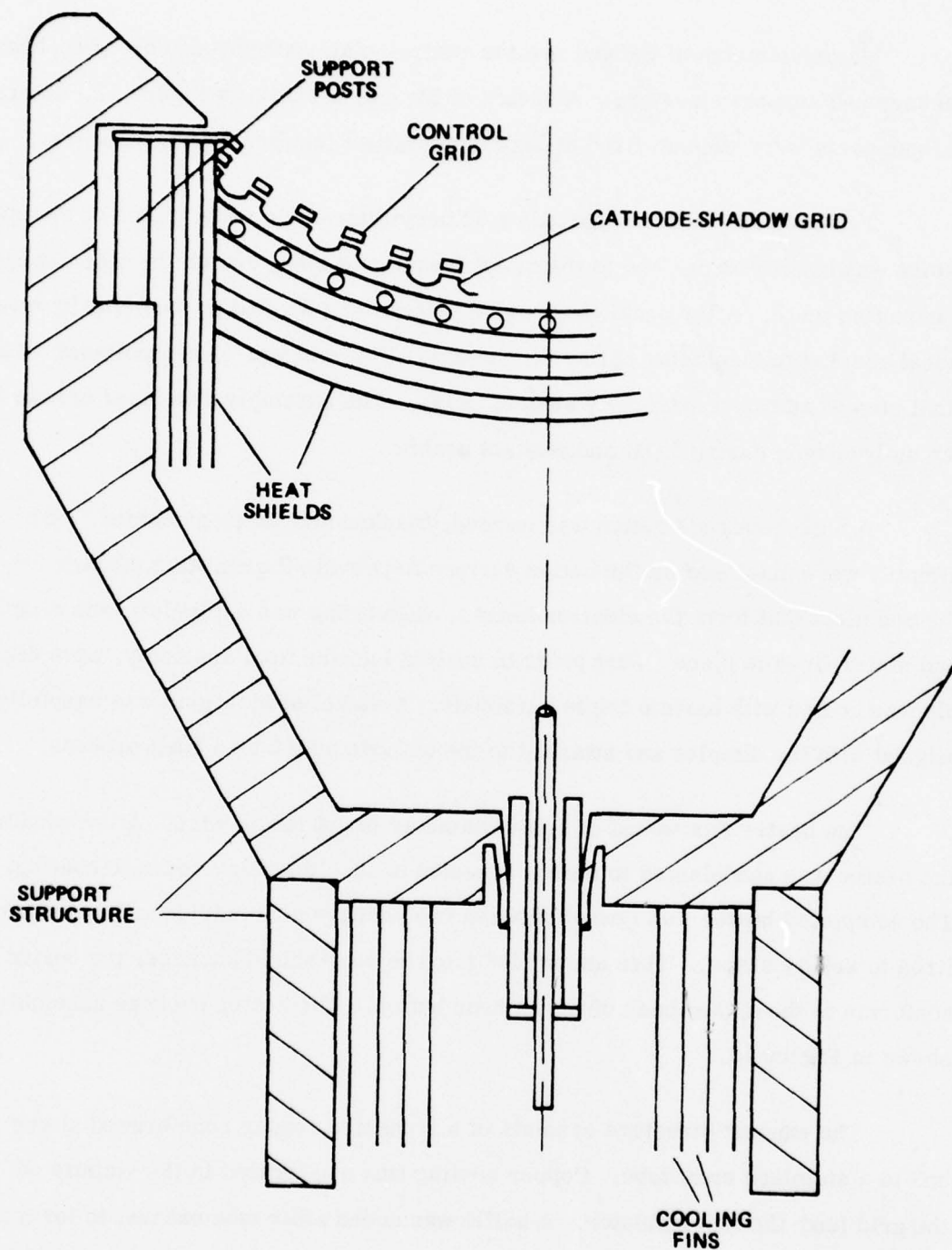
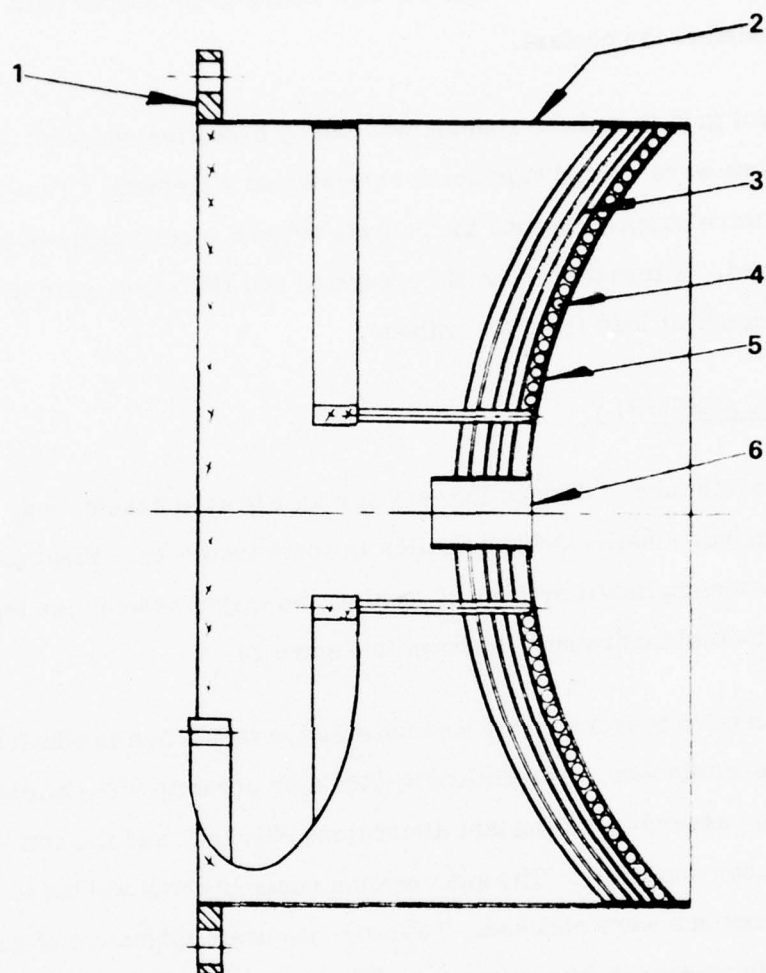


Figure 12. Gun Sketch
20



- 1 - HEATER SUPPORT RING
- 2 - HEATER CYLINDER
- 3 - HEAT SHIELD
- 4 - HEATER COIL
- 5 - PERFORATED HEAT SHIELD
- 6 - ROLLED SLEEVE

Figure 13. Heater Package Assembly

inside surface of the reentrant stainless steel support tube. Conduction heat loss from the gun elements flows through the high conductance copper path to the fins and is dissipated in the coolant.

Control grid to cathode spacing was set by precision spacers. Adjustable support sleeves were welded together for permanent alignment. Thin molybdenum heat shields were wrapped around the cathode support sleeve prior to assembling the control grid. Alternate layers of corrugated and flat stock were used to minimize conduction heat loss from the cathode.

C. FINAL ASSEMBLY

The switch tube is divided into seven major brazed assemblies. Major assemblies include smaller subassemblies in some instances. Final tube construction was accomplished by Heliarc welding the major assemblies together. The switch tube outline drawing is shown in Figure 14.

The massive body assembly was used as the foundation to which the other assemblies were attached. The collector-insulator ceramic was attached to the collector-probe assembly, important dimensions checked, and the entire unit attached to the body assembly. The gun ceramic assembly was welded to the body and more dimensions were checked. To insure accurate alignment of gun and anode, a precision spacer that indexed on the anode and focus electrode inside diameters was positioned and the gun-to-baseplate weld was made. After removal of the spacer, the baseplate to ceramic weld was made.

A 8 l/sec VacIon[®] pump was attached as a final step. An improved VacIon pump and magnet assembly has been used in place of the bulky pump, magnet and shield combination used on earlier switch tubes. The new package is specified at nominal dimensions of 5.25 in x 6 in x 3.13 in (exclusive of insulator and tubulation) and weighs only 9 pounds. Figure 15 gives dimensions and specifications of the improved package.

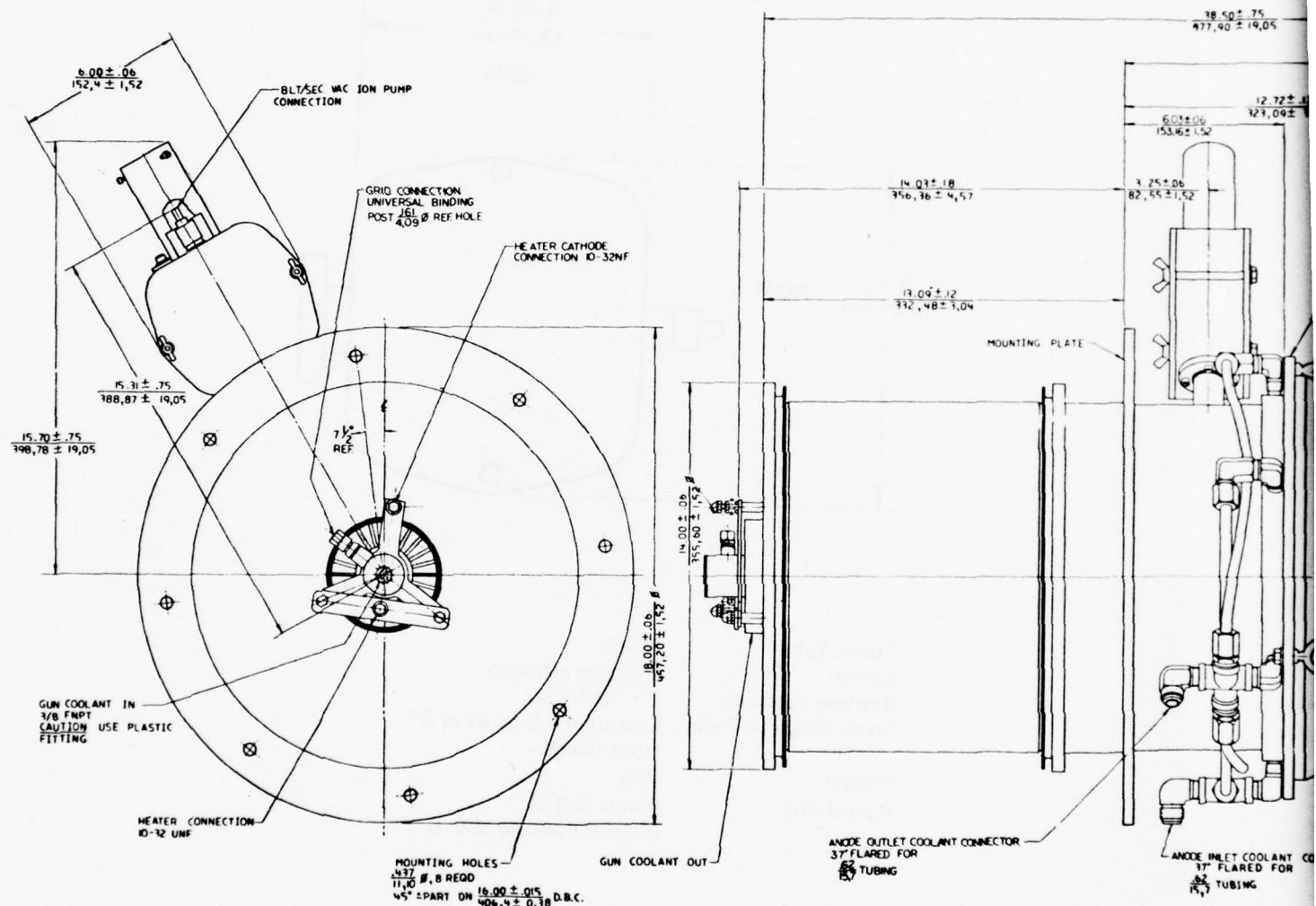
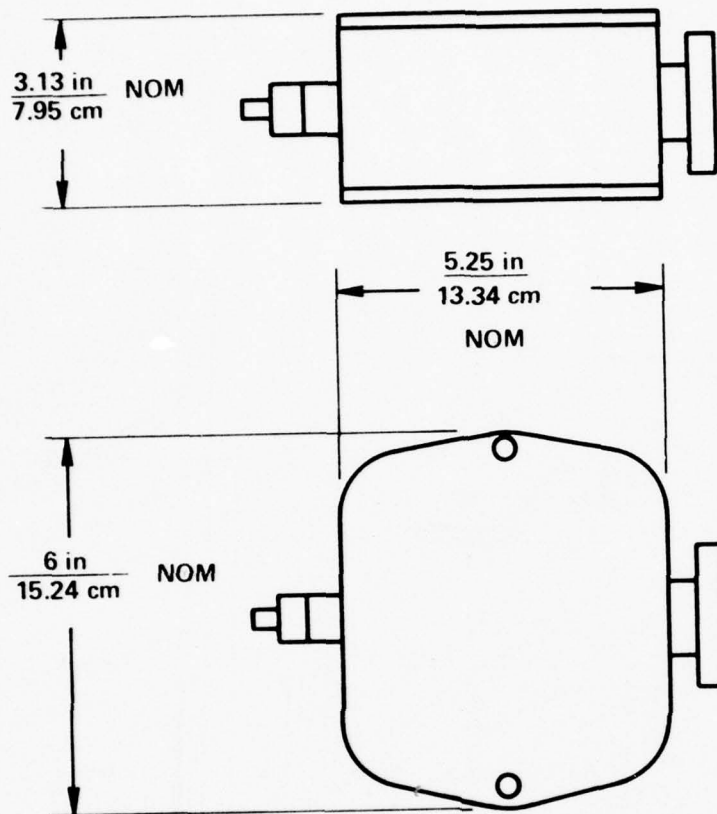


Figure 14. VKW-8253C

2		1	
DATE	DESCRIPTION	AMOUNT	BALANCE
A - 100.00		100.00	
B - 100.00		100.00	
C - 100.00		100.00	



(A)



Pump Type	Diode
Speed:	8 l/s for nitrogen
Starting Pressure:	1×10^{-2} Torr
Stray Magnetic Field:	Less than 1/2 gauss at 3" from flange
Weight:	9 lb
Bakeability:	Pump 550°C
	Magnet Package 350°C

Figure 15. Shielded VacIon® Pump

III. EXHAUST AND HIGH POT

After final assembly and leak check, the tube was mounted on an exhaust-bakeout station. The tube was pumped with a diffusion pump backed by a forepump. Valves are provided to attach a leak detector when required. Pressure was recorded on a printout from the ionization gauge control. Thermocouples were attached to various parts of the tube to control and monitor tube temperature.

The space inside the oven that surrounds the tube was evacuated to prevent oxidation during high temperature bakeout. A port is provided for introducing helium for leak detection. A system of three forepumps was used to pump this region.

Total bakeout time, not including warm-up and cool-down time, was 55 hours. Bakeout temperature was 450° C.

After bakeout, the cathode was converted. Forced-air cooling was provided by directing a blower at the gun. Starting at 3 volts, the heater voltage was slowly increased over a 3-hour period until conversion was reached at approximately 23 volts. The tube was heater-aged overnight and sealed off the vacuum pump in the morning. The grid circuit was high-potted to reduce leakage current. Heater aging continued for another week, with interruptions for tube dress.

The tube was installed in the test station with all monitoring equipment in place so that after high-potting, high power testing could start without interruption for test set modification. The entire tube was submerged in the shielded oil tank.

Electrodes and ceramic insulators were conditioned using a high voltage, high impedance, dc power supply. Of the two high voltage ceramics, the collector insulator encounters the least severe operating conditions. Potential deposits that may evolve from the gun are effectively masked by the massive anode structure.

Further, the video voltage goal of 140 kV at a duty cycle of 0.03 (0.08 goal) is a far less severe standoff requirement than the 165 kVdc design goal for the gun. The collector ceramic was effectively dc high-potted without exceeding 5×10^{-8} Torr.

As expected, the major high-pot effort was expended on reducing leakage current on the gun ceramic. Results were quite encouraging. Starting at 50 kV, the voltage was raised in 10 kV steps to 200 kVdc. Time at each voltage was determined by leakage current and gas level. Gas pressure was kept under 5×10^{-7} Torr during the entire process.

At the conclusion of high voltage processing, high-pot current was $60 \mu\text{A}$ at the specification goal of 165 kVdc standoff.

IV. PRELIMINARY TESTING

The reduced power capability of the breadboard model switch tube was demonstrated in tests performed at Varian in late May and early June 1977. Test power level was limited primarily by the capacitor ratings of the power supply. 100 kV video output at a 0.03 duty cycle was reached briefly before successive failure of capacitors made operation at lower power levels necessary. At this point, testing was limited to a maximum supply voltage of 88 kV. No further power supply problems were encountered even when operating at a pulse width of 300 μ sec.

Figure 16 is a simplified drawing of the test setup. The switch tube was mounted in a horizontal position in a shielded oil tank. Forced oil from a submergible pump was used to cool the reentrant gun structure. In the event of vertical mounting, the reentrant gun structure must be vented to bleed off trapped air as the oil tank is filled.

An S-band microwave tube was used as the load. Nominal perveance of the load tube was 1.94 μ perv. The load tube was installed in a shielded enclosure adjacent to the switch tube, and the two tubes used a common oil tank.

The collector, probe and body coolant circuits were fitted with thermocouples and calibrated flowmeters to determine power dissipation in different sections of the tube. Nominal water cooling flow rates for these tests were: collector flow, 23 gpm; probe flow, 5 to 10 gpm; and body flow, 5 to 10 gpm. For operation at higher power levels, or with coolant other than water, increased flow rates will be necessary. Figures 17, 18, and 19 give flow versus pressure drop data for each of the circuits.

Heater power requirements were evaluated at voltage settings between 19 and 20 V. After initial evaluation, a heater power of 450 W (20 V, 22.5 A) was used for all tests. Figure 20 is a plot of heater current versus voltage in the range of interest.

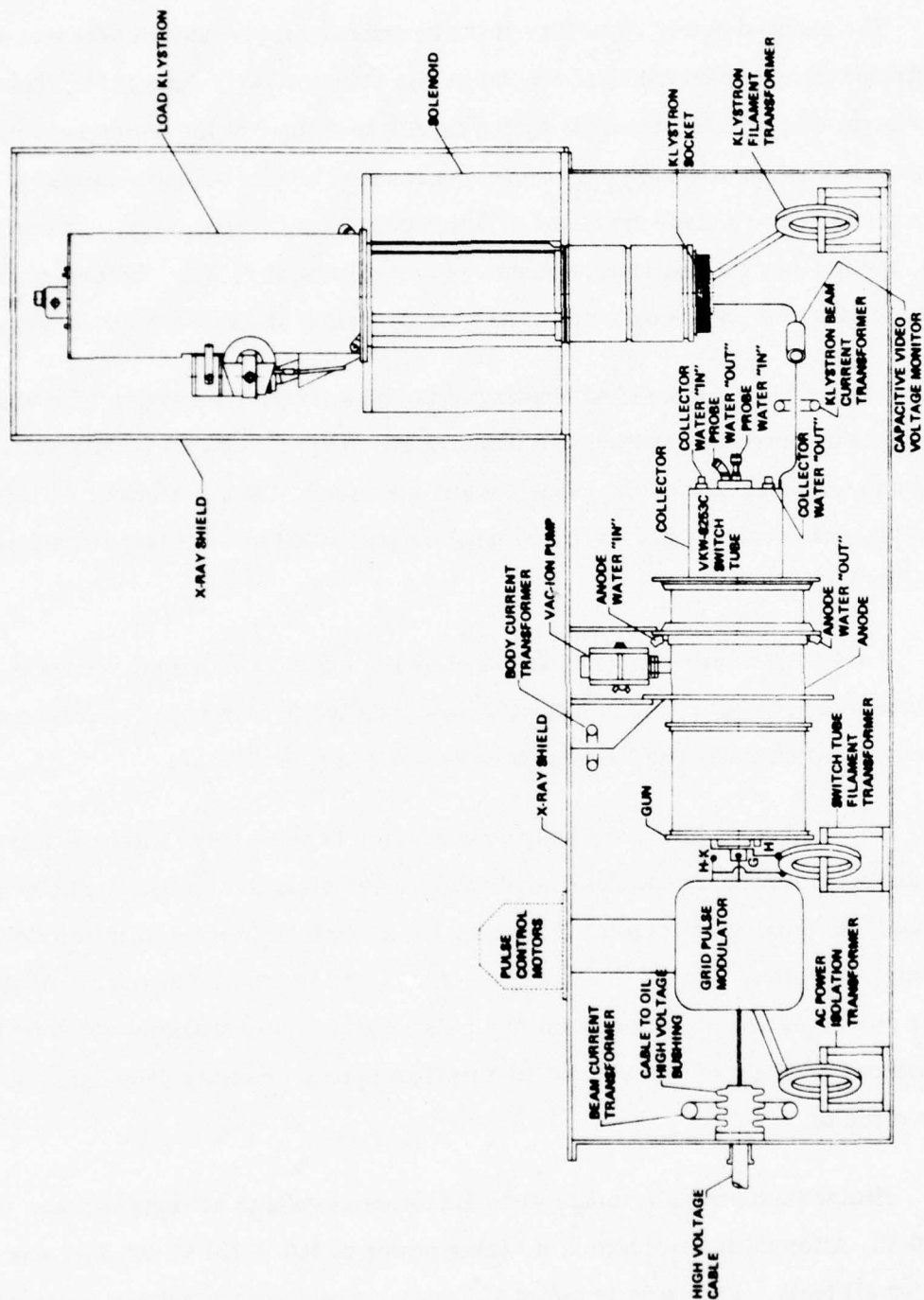


Figure 16. Simplified Modulator Layout Sketch

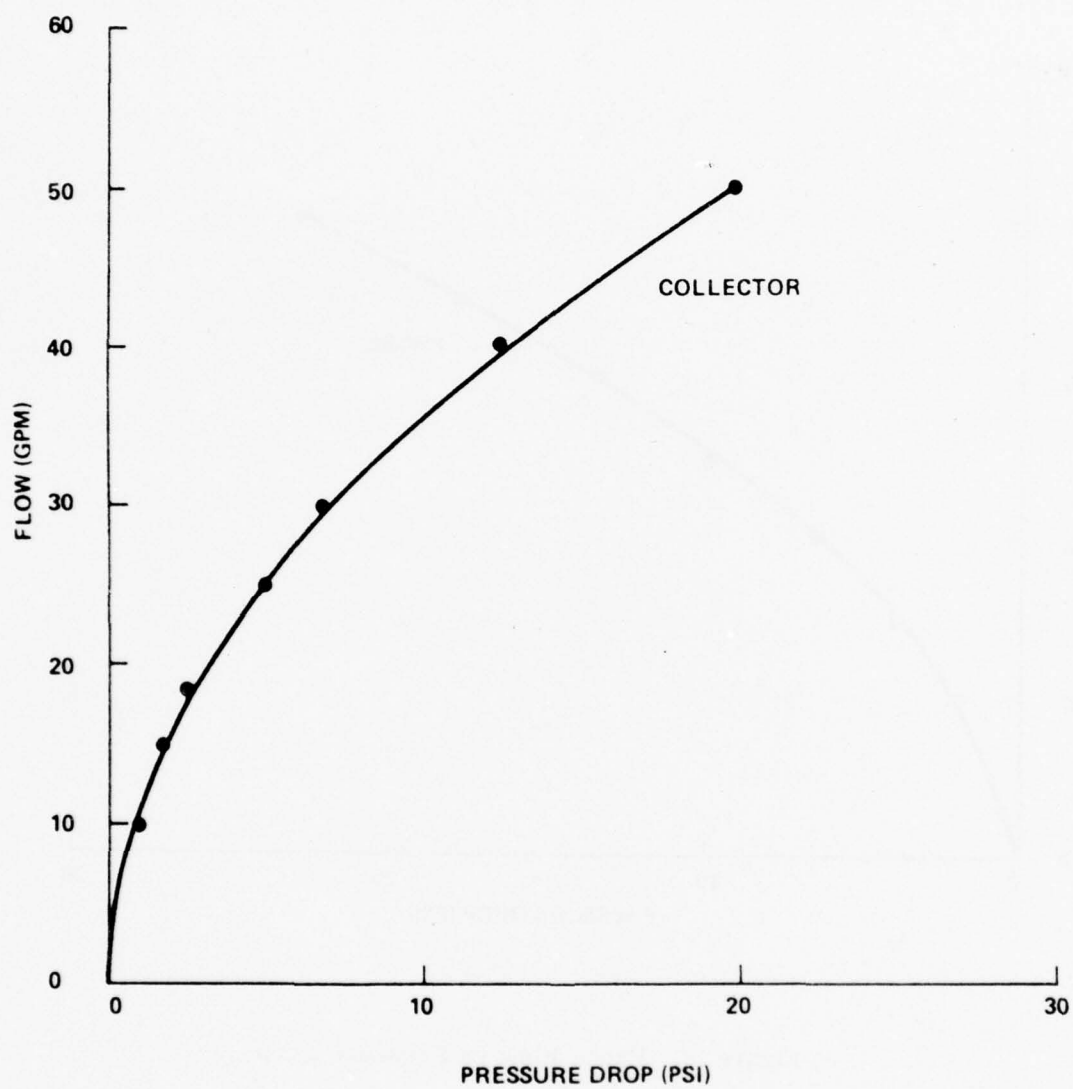


Figure 17. Collector Flow vs Pressure Drop

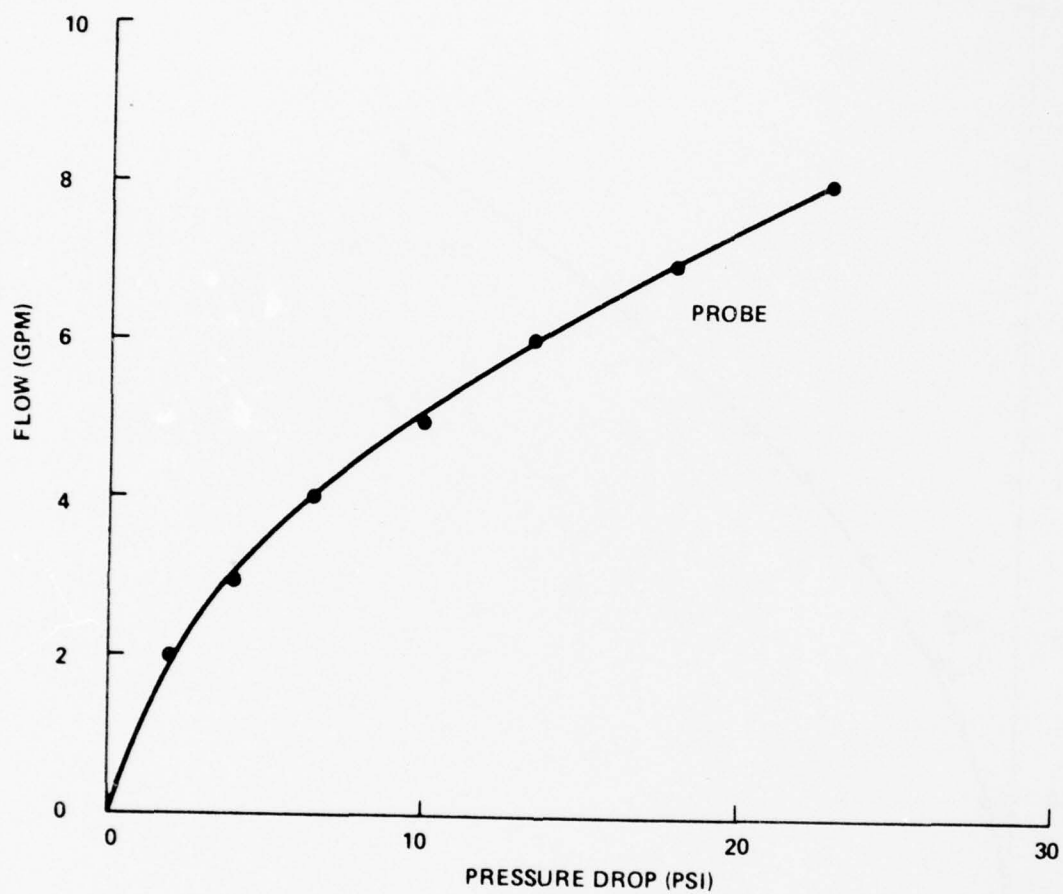


Figure 18. Probe Flow vs Pressure Drop

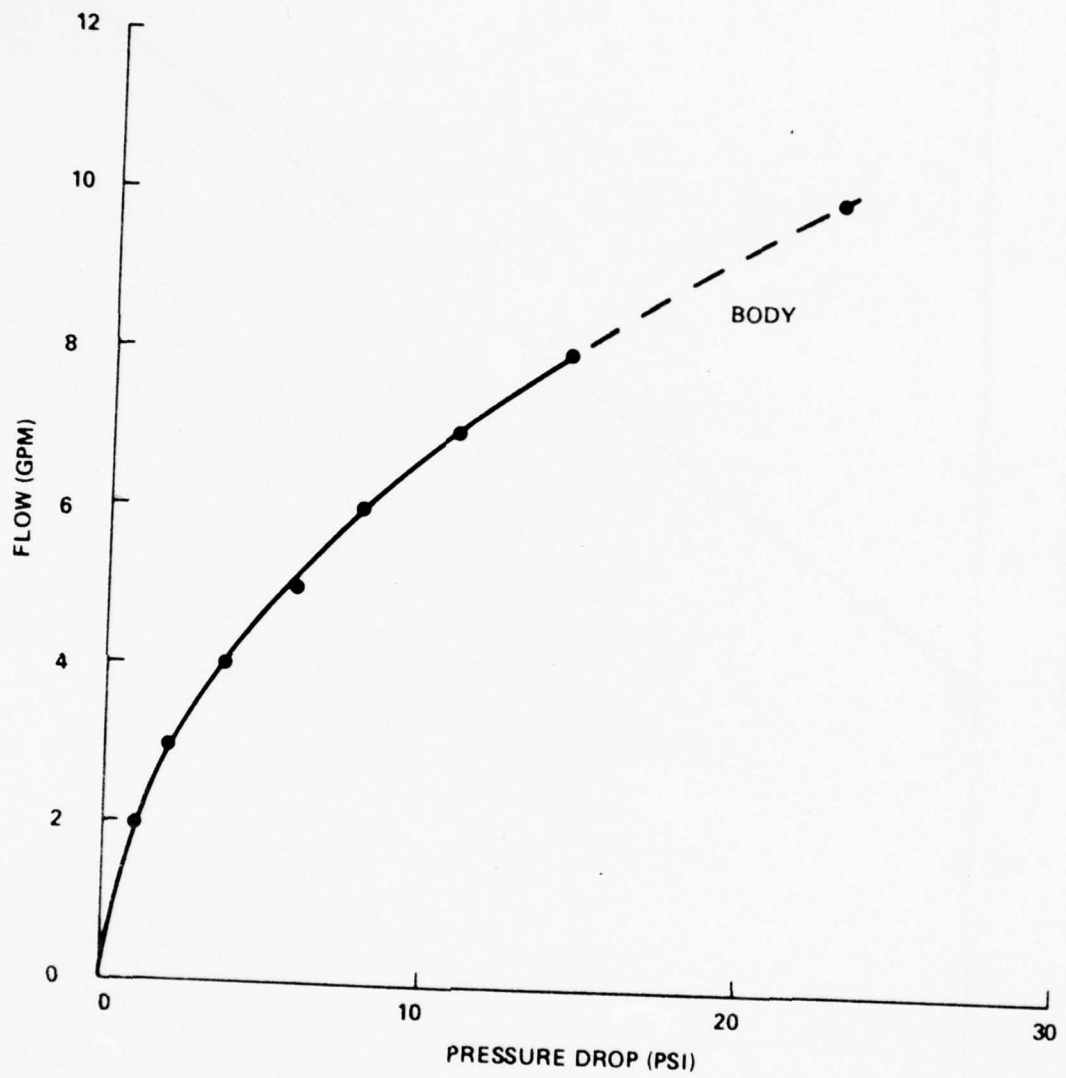


Figure 19. Body Flow vs Pressure Drop

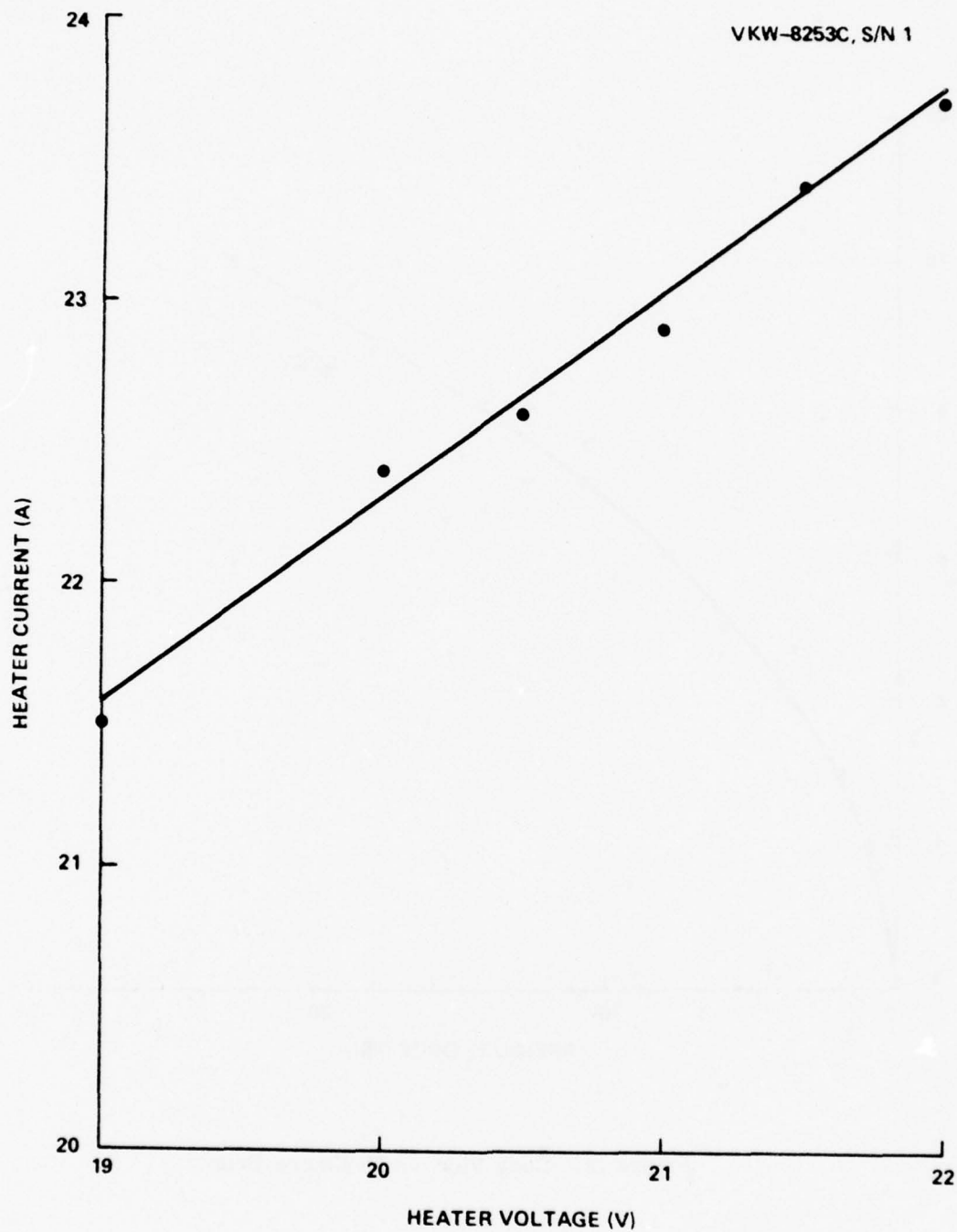


Figure 20. Heater Current vs Heater Voltage

Current transformers were used to monitor cathode, anode and load tube current. A capacitance divider, attached to the switch tube collector, was used to measure video output voltage. Switch tube cathode voltage was determined by reading the supply voltage and accounting for the IR drop during on-time.

Collector, body and probe dissipation measurements were made at three different power levels, as shown in Figures 21, 22 and 23. Figures 24, 25 and 26 show the same data in terms of collector depression. Power supply failure prevented completion of the high-power test run plotted in Figures 23 and 26. The dotted portions of the curves have been extrapolated from other test data.

The body power has been added to the collector power for comparison with data taken on the switch tube described earlier. Beyond 95% depression, the curves again show the sharp increase in body power attributed to reflected electrons. This is graphically demonstrated in Figure 27, which shows the actual division of collector, probe and body power in a typical case.

The maximum probe-collector dissipation again occurred at 60% depression. As mentioned earlier, this result had been predicted by mathematical analysis.

Ratios of probe power to total power at 88 kV and 99 kV are shown in Figure 28. Ratios fell between 0.15 and 0.3 as on the earlier tube.

Figure 29 is a comparison of VKW-8253B and VKW-8253C dissipation ratios at the 88 kV level. Corresponding data were not taken at the 108 kV level due to power supply limitations. The division of probe and collector power was similar in both tubes. These results are encouraging, since the improved probe geometry seems to provide enhanced cooling without penalty of increased beam interception.

Dynamic impedance was measured as a function of cathode voltage at two different video output voltages, as shown in Figures 30 and 31. Grid drive remained constant for the measurements.

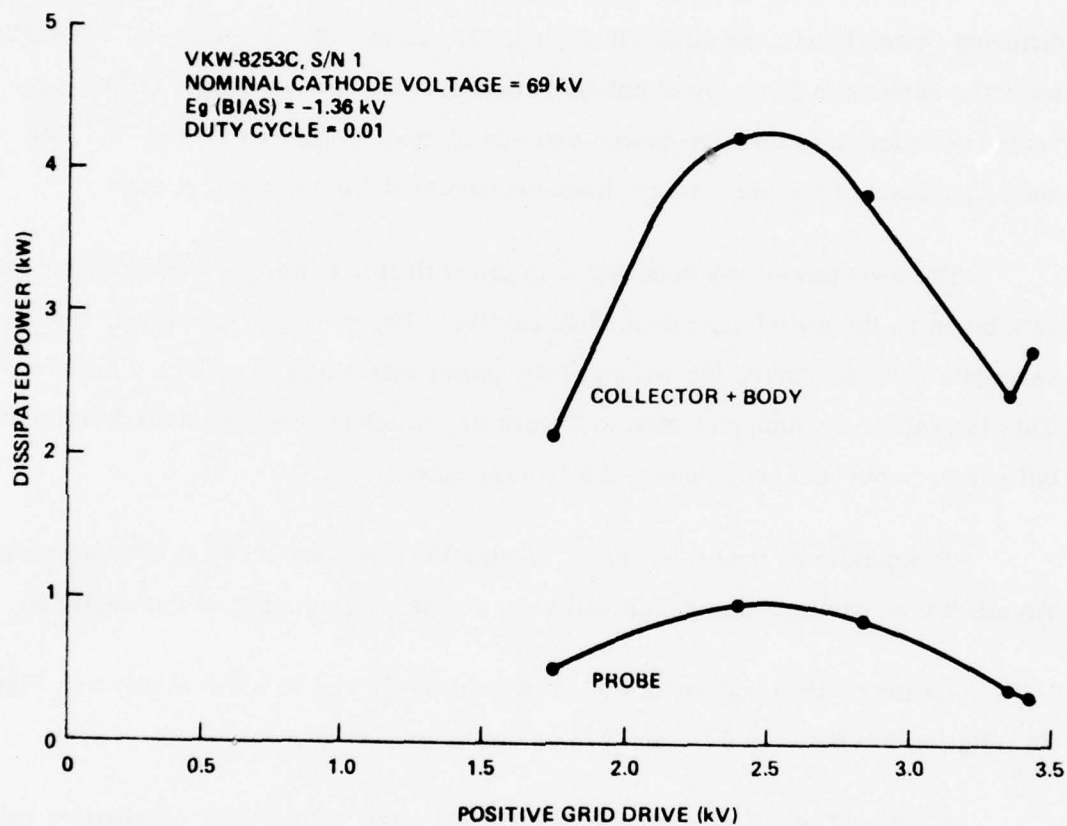


Figure 21. Dissipated Power vs Grid Drive at 69 kV

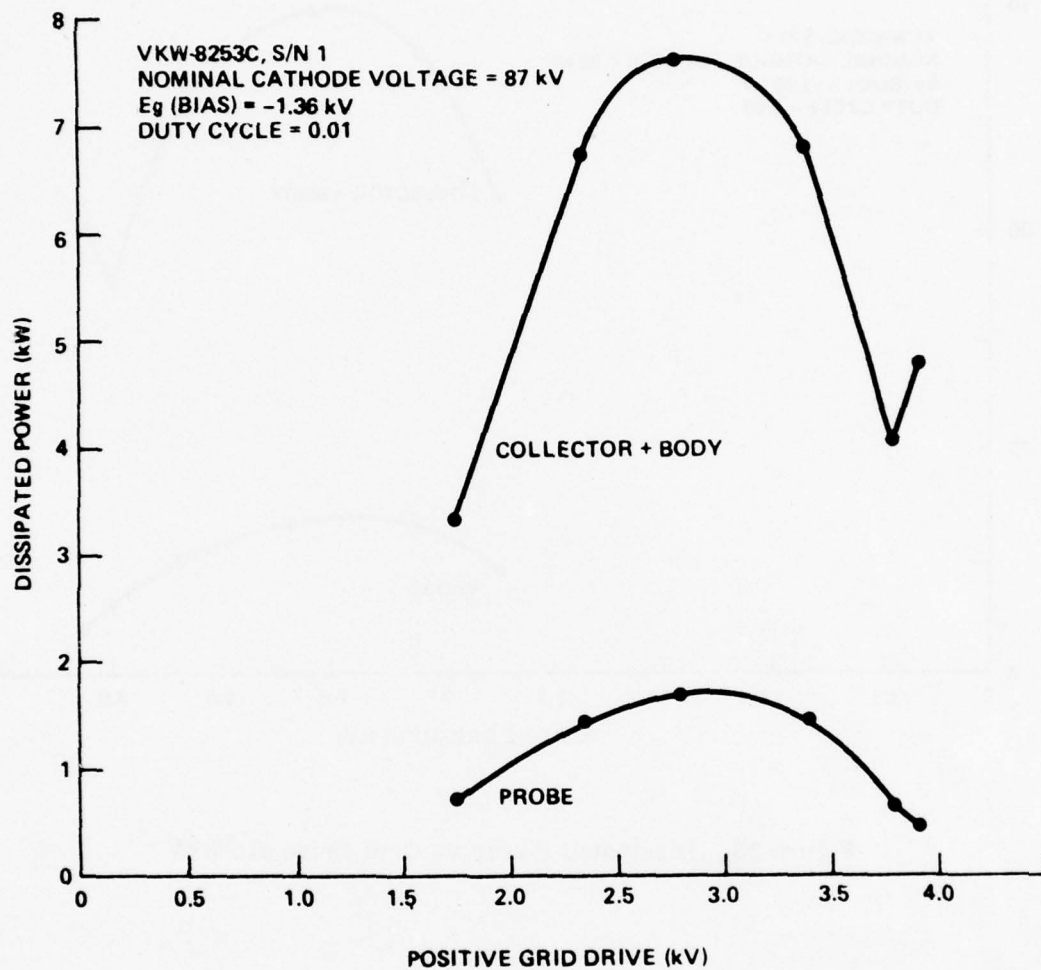


Figure 22. Dissipated Power vs Grid Drive at 87 kV

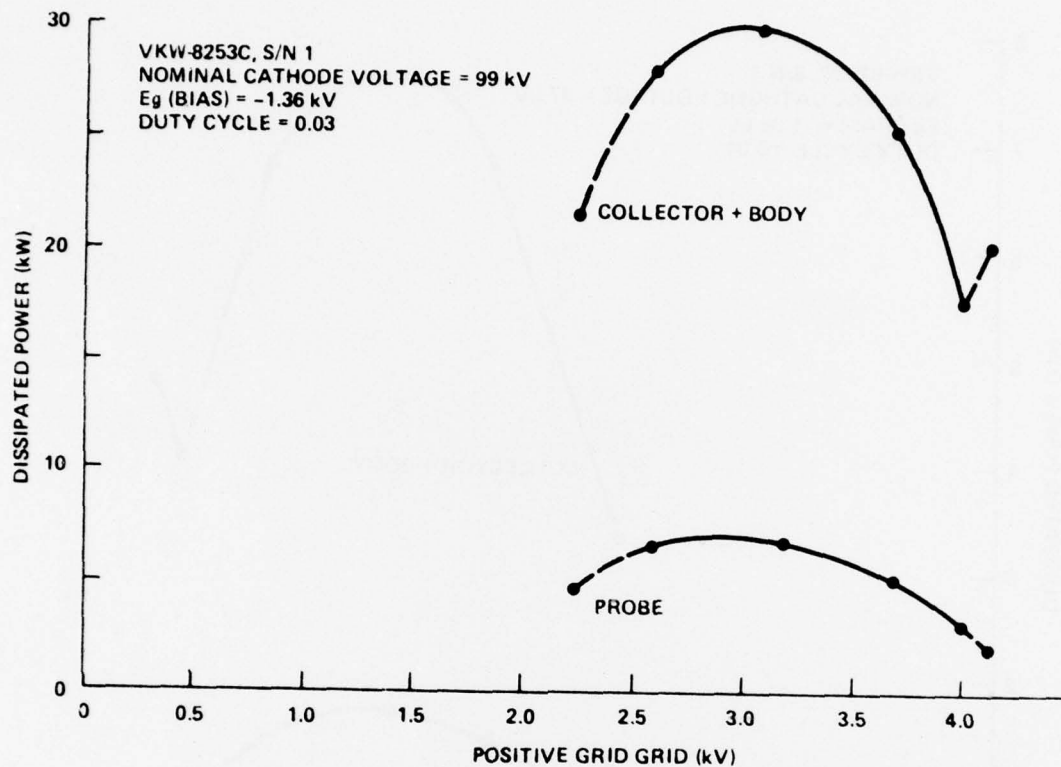


Figure 23. Dissipated Power vs Grid Drive at 99 kV

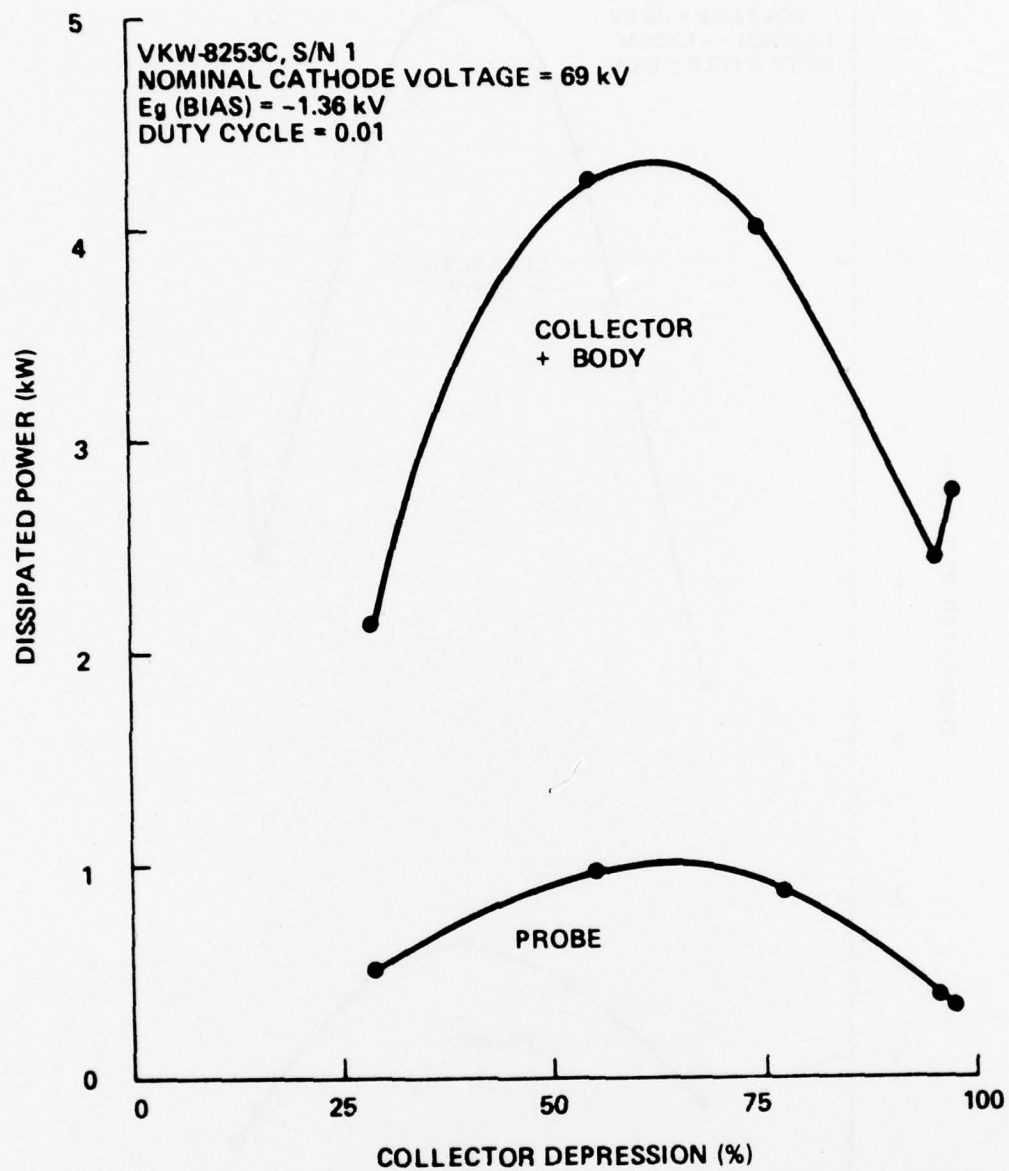


Figure 24. Dissipated Power vs Collector Depression at 69 kV

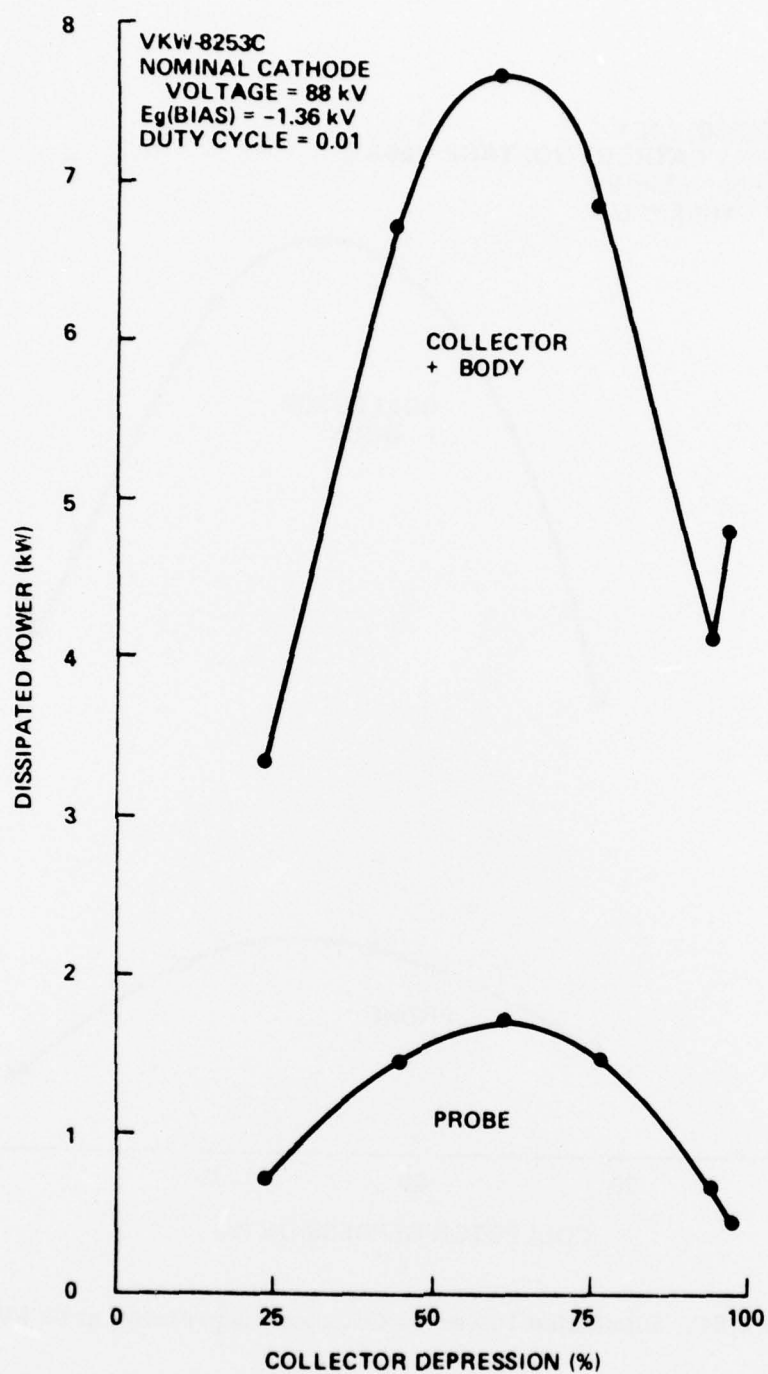


Figure 25. Dissipated Power vs Collector Depression at 88 kV

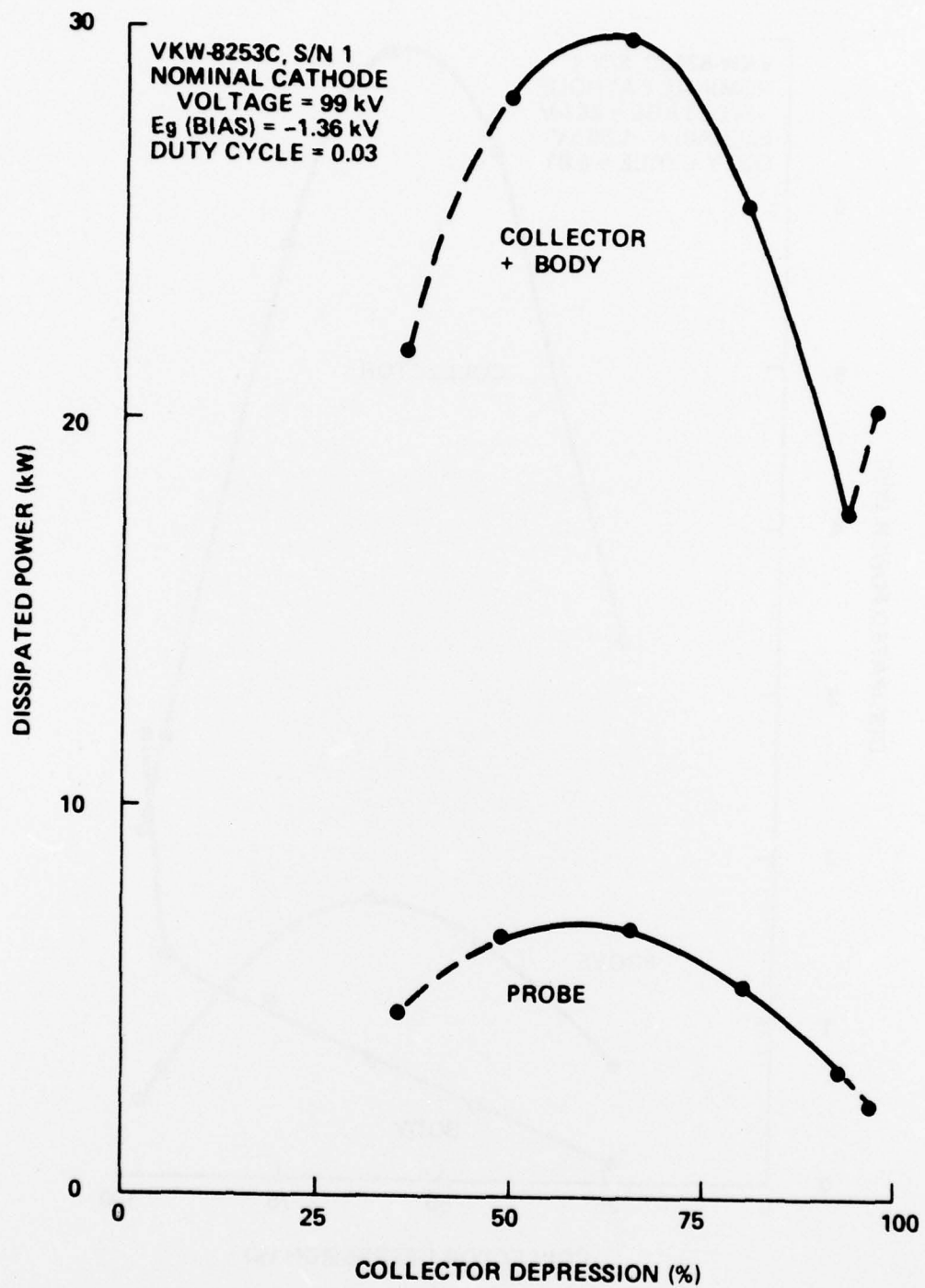


Figure 26. Dissipated Power vs Collector Depression at 99 kV

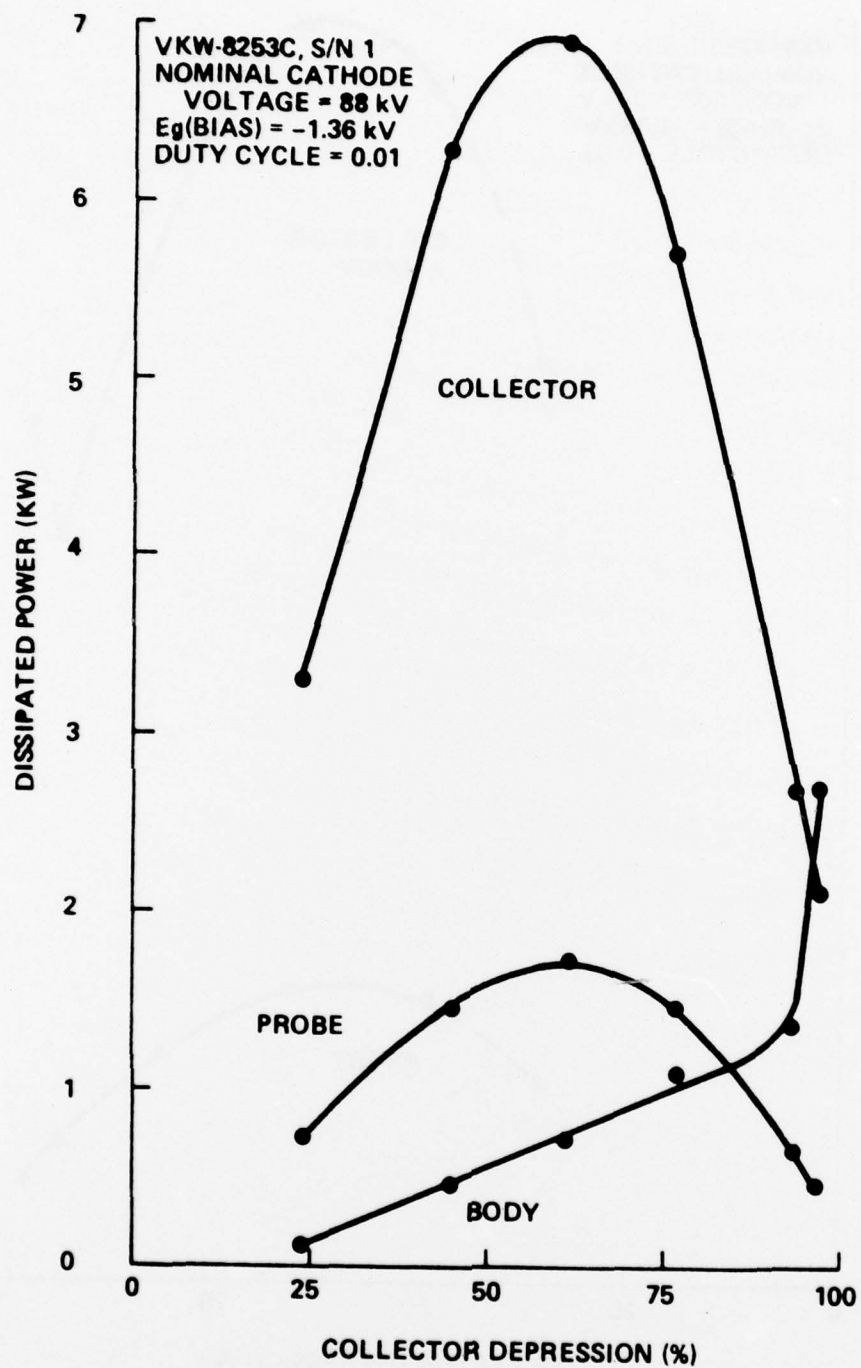


Figure 27. Collector, Probe, and Body Power vs Collector Depression

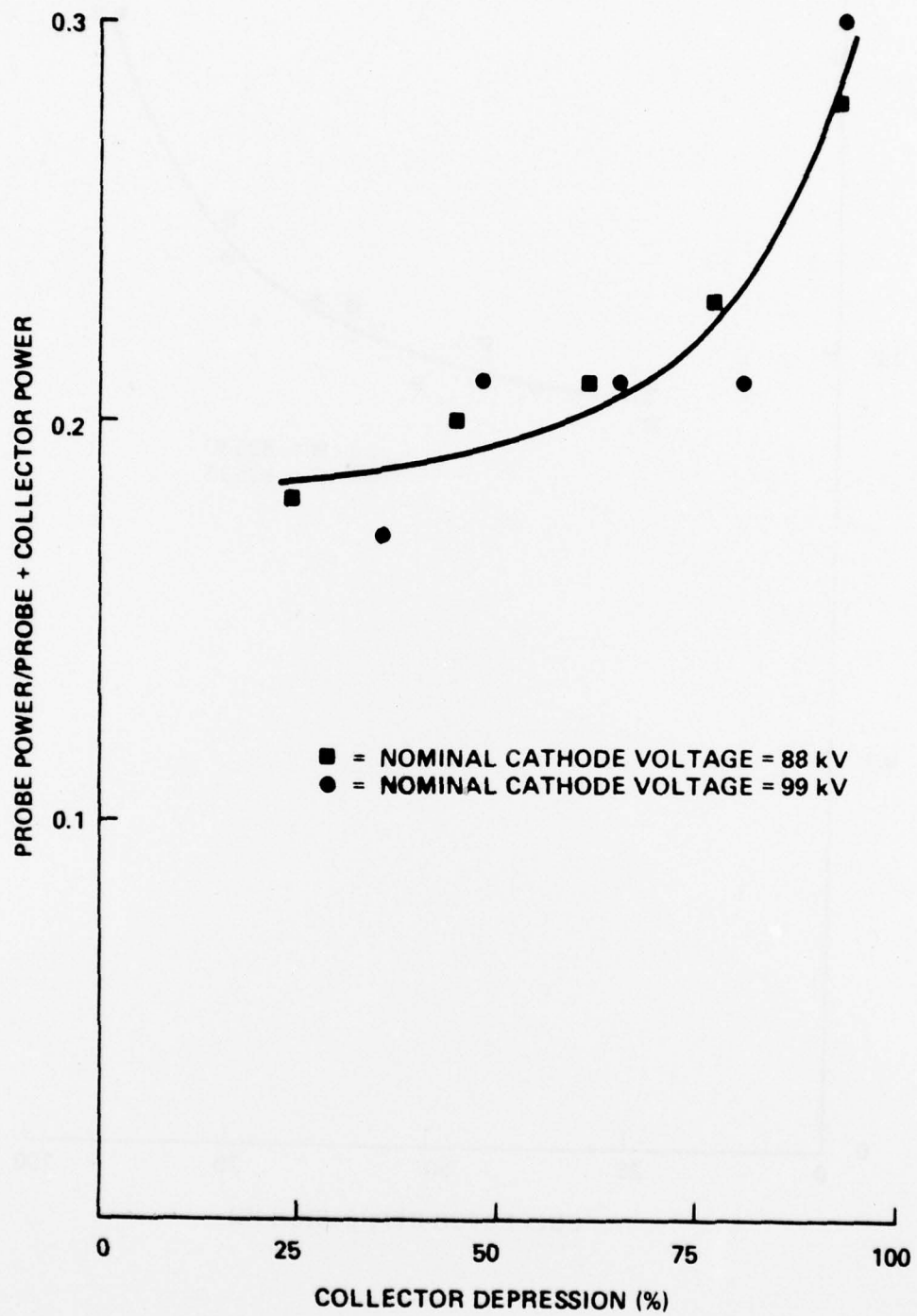


Figure 28. VKW-8253C Probe Power vs Collector Depression

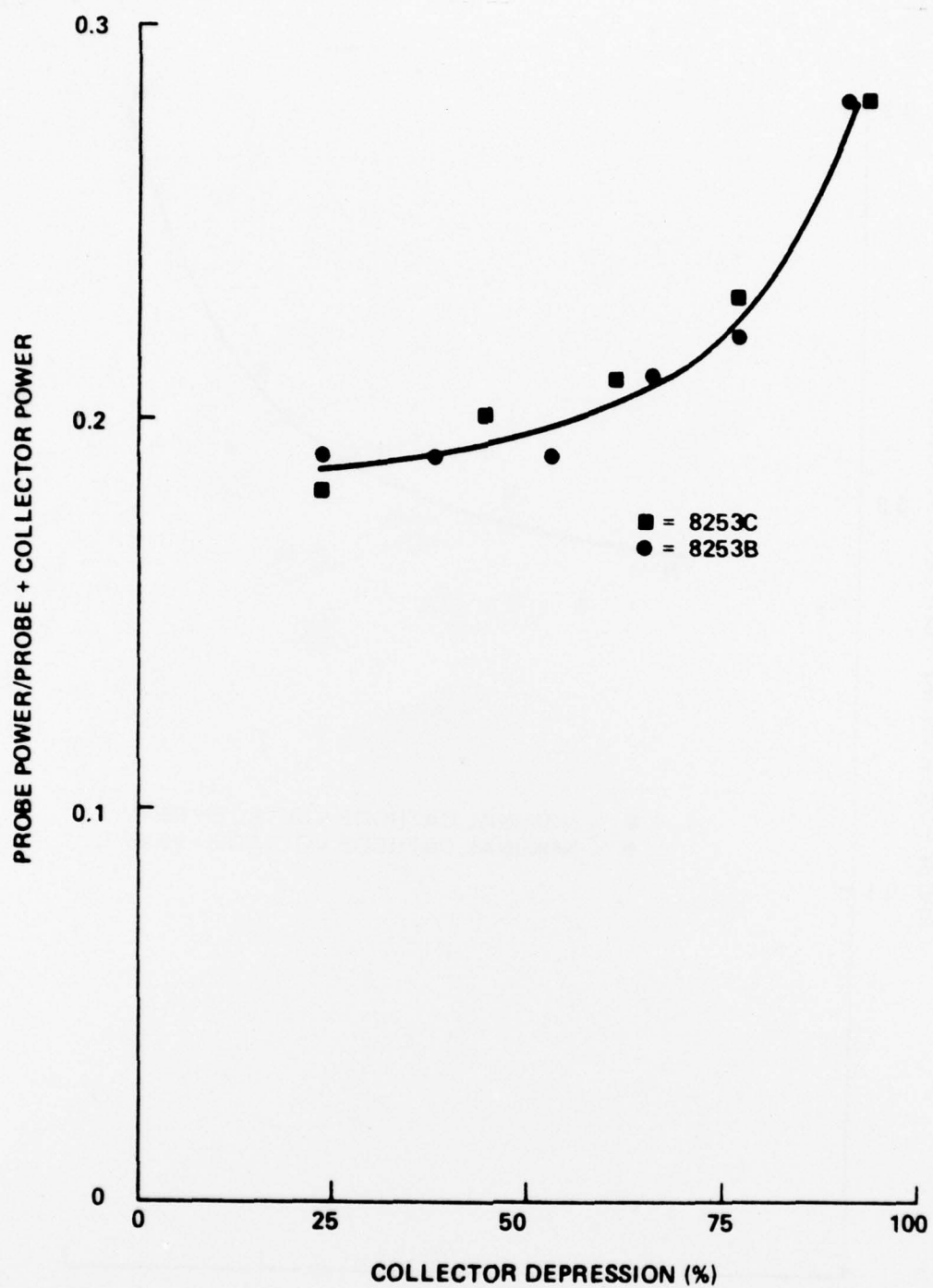


Figure 29. VKW-8253B and VKW-8253C Probe Power vs Collector Depression

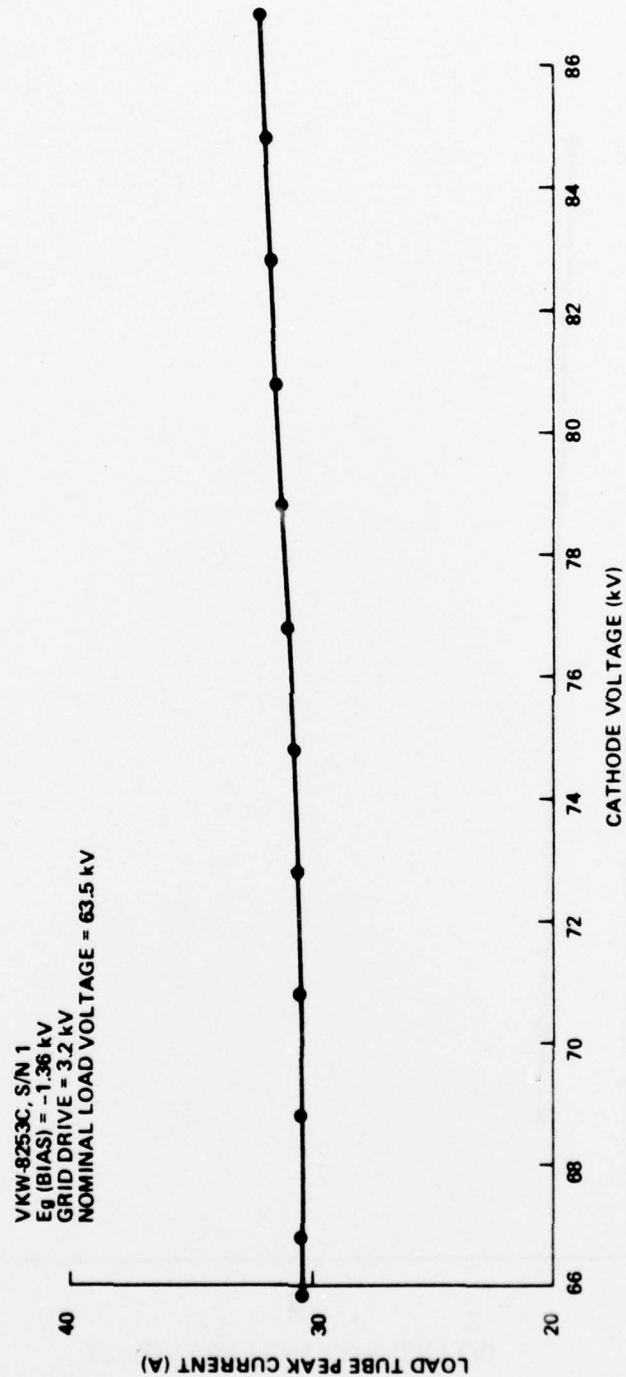


Figure 30. Dynamic Impedance at 63.5 kV

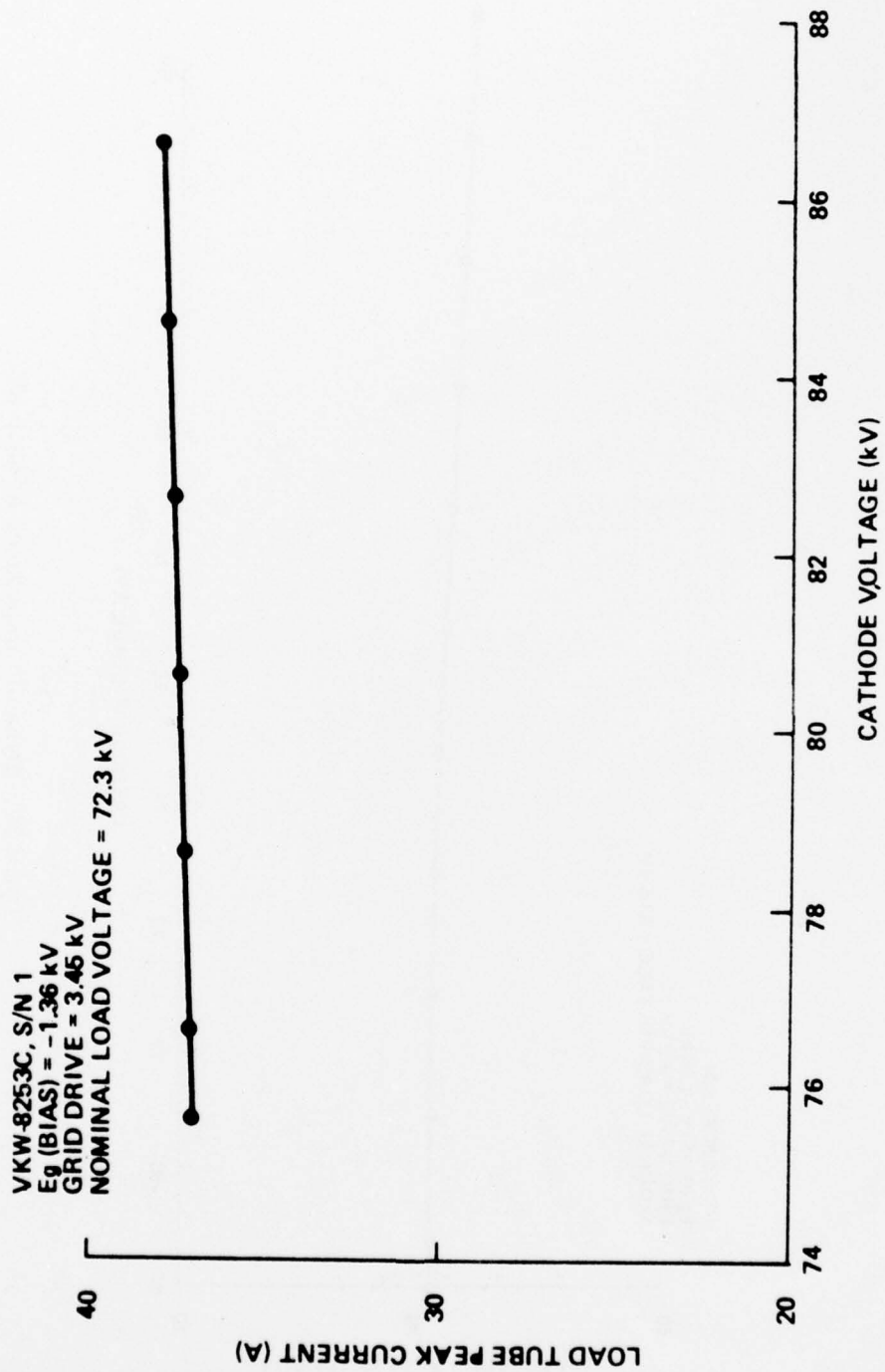


Figure 31. Dynamic Impedance at 72.3 kV

At a nominal video output level of 63.5 kV, the average dynamic impedance was 12 k Ω for a beam voltage variation of 21 kV (collector depression in the range 94.5% to 74.7%). At a nominal video level of 72.3 kV, comparable values were an average impedance of 11 k Ω for a beam voltage variation of 11 kV (depression in the range 95% to 84%). Impedance was expected to vary with beam voltage, but available metering did not provide the resolution necessary to calculate other than an overall average value.

Grid drive characteristics at two different cathode voltages are shown in Figures 32 and 33.

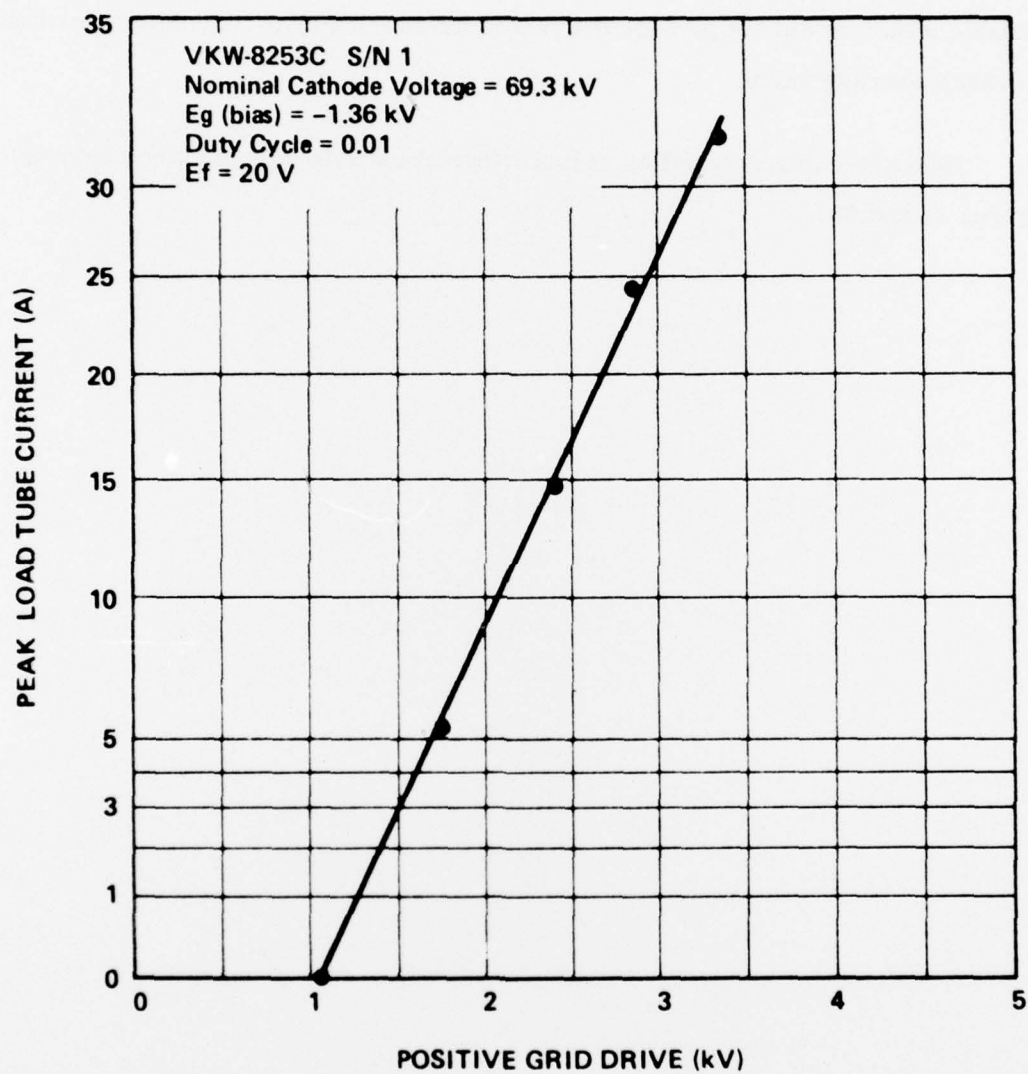


Figure 32. Load Tube Current vs Grid Drive at 69.3 kV

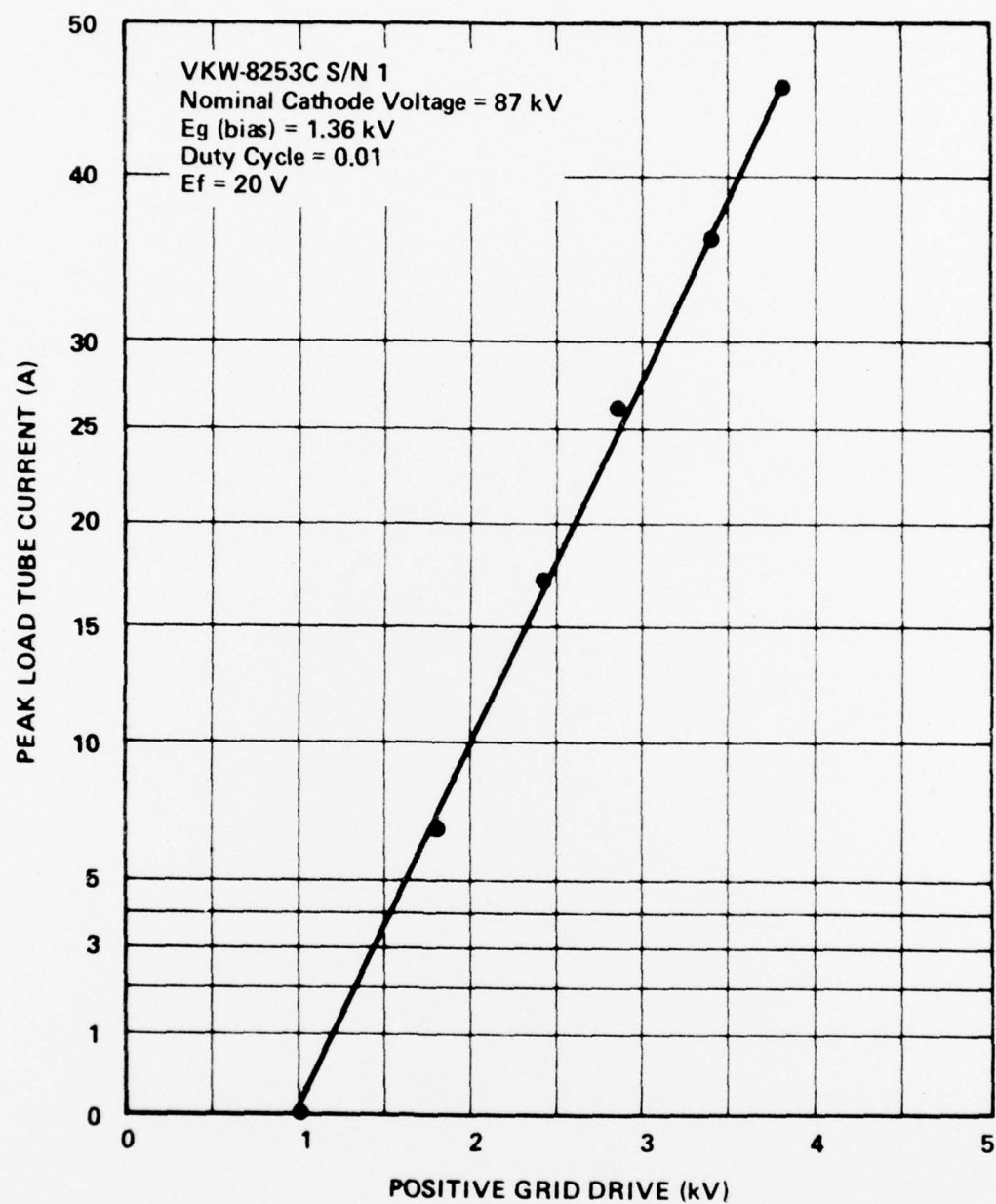


Figure 33. Load Tube Current vs Grid Drive at 87 kV

V. CONCLUSIONS AND RECOMMENDATIONS

The switch tube with the improved collector-probe system was tested at reduced power levels at Varian prior to delivery to RADC. Its performance characteristics were similar to those of the earlier model VKW-8253B switch tube. We expect equivalent performance at higher voltage and power levels.

At the levels tested, maximum efficiency was reached at approximately 95% collector depression. This was also the point of minimum collector-probe dissipation (although dissipation will continue to drop as 100% depression is approached). The preferred point of operation should be about 90% depression, however, to avoid the sudden increase in body power as saturation is reached. At the lower depression level, the increase in collector-probe power is not significant and the efficiency is reduced by only about four percentage points.

We expect the collector-probe system to perform satisfactorily at the specification goals of 140 kV, 100 A, video output at a duty cycle of 0.05 (about midway between the min - max design goal of 0.03 - 0.08) and at the recommended 90% depression level, subject to the following reasoning.

Based on our reduced power experiments, we estimate that the probe will dissipate 26% of the combined collector-probe power. This corresponds to 19.5 kW average under the stated conditions. For our estimates, we make the simplification that all the beam interception will take place in the forward one-half of the probe, although it is recognized that interception actually will be greatest at the tip and drop off rapidly along its length. The resulting average power density is less than 0.200 kW/cm^2 over that area. The peak power involved is not great enough to cause pulse heating to be a factor even at pulse lengths up to 300 μsec . A minimum water flow of 10 gpm should be maintained through the probe.

Using a similar analysis on the collector, we estimate that the collector will dissipate 55.5 kW under the same operating conditions. Again using the same simplification of one-half effective surface area, the average power density is less than that calculated for the probe. We recommend a minimum collector flow rate of 35 gpm. Body power should be monitored to assure that body heating does not become a consideration as the higher power levels are reached. Recommended body flow rate is 10 gpm.

Operating conditions more severe than those described should be approached with caution. The collector is capable of higher power levels, but extreme power densities at the probe tip may become the limiting factor. Increased water flow rates should be used in any event.

No X-ray, or rf shielding has been added to the tube. It is the users responsibility to provide shielding and interlocks. Tube hazards are described in the Preliminary Hazard Analysis dated September 28, 1976 that was submitted to RADC on this contract.

Interest in a 200 kV linear beam switch tube has grown in recent years. Early design effort was directed toward development of a reliable tube in the 120-130 kV range at modest duty cycles. We believe that experience gained in design of the intermediate power device described in this report, particularly in the area of collector design, can lead to an operational 200 kV device.

MISSION *of* **Rome Air Development Center**

RADC plans and conducts research, exploratory and advanced development programs in command, control, and communications (C³) activities, and in the C³ areas of information sciences and intelligence. The principal technical mission areas are communications, electromagnetic guidance and control, surveillance of ground and aerospace objects, intelligence data collection and handling, information system technology, ionospheric propagation, solid state sciences, microwave physics and electronic reliability, maintainability and compatibility.

